J. Fluid Mech. (1986), *vol.* 168, *pp.* 89–117
Printed in Great Britain

Internal waves, fossil turbulence, and composite ocean microstructure spectra

By CARL H. GIBSON

Departments of Applied Mechanics and Engineering Sciences, *and* Scripps Institution of Oceanography, University of California, San Diego, La Jolla, CA 92093, USA

(Received 4 January 1984 and in revised form 9 December 1985)

Composite vertical shear spectra of Gargett *et al.* (1981) and composite vertical temperature-gradient spectra of Gregg (1977) are compared with the fossil-turbulence model of Gibson (1980–6). Both the shear and temperature-gradient spectra show high-wavenumber microstructure bumps which are identified by Gargett *et al.* (1981) and Gregg (1980) as due to turbulence in the fluid at the time of measurement. However, using $\gamma \geqslant 5N$ as the criterion for turbulence to exist in a stratified fluid, where γ is the rate of strain and N is the Brunt–Väisälä frequency, the largest-scale fluctuations of the microstructure bumps may actually be remnants of previous turbulence persisting in fluid that is no longer turbulent at these scales: such fluctuations are termed fossil vorticity turbulence (a class of internal waves) and fossil temperature turbulence respectively. Both composite spectra exhibit k^{-1} subranges which are identified by their low amplitudes as subsaturated (two–three)-dimensional internal waves and resulting temperature fine structure by comparison with saturated three-dimensional internal-wave subranges proposed by Gibson (1980): $7N^2k^{-1}$ for the saturated vertical shear spectrum and 0.7 $(\partial\overline{T}/\partial z)^2 k^{-1}$ for the saturated temperature gradient spectrum. Both composite spectra exhibit a transition between k^{-1} and k^0 subranges at wavelengths of 6–14 metres: possibly a fossil remnant of previous overturning turbulence which produced 3–7 m thick partially mixed layers. Dissipation rates ϵ and χ and Cox numbers $C \equiv (\overline{\nabla T})^2/(\nabla\overline{T})^2$ of the turbulence required by this assumption are much larger than the measured values, suggesting that the turbulence process has been undersampled. Fossil overturning scales up to about 10 m are indicated by the Gregg (1977) data. Average (150 m) C values $\bar{C}$ are distributed as a very intermittent lognormal, with variance $\sigma^2_{\ln \bar{C}} = 5.4$, also indicating extreme undersampling of the turbulence and mixing.

1. Introduction

Measurements of fluctuating velocity and temperature fields on vertical scales from 10^2 to 10^{-2} m in the ocean have recently become available. Studies of these data may lead to a better understanding of the coupling between large-scale processes such as internal waves and small-scale processes such as turbulence which do the mixing and vertical diffusion of temperature and chemical species concentration. A review of the available ocean data and some of the theoretical interpretations may be found in Munk (1981).

The purpose of the present paper is to compare composite spectral forms of Gargett *et al.*(1981) and Gregg (1977) from the main thermocline of the Atlantic and Pacific oceans respectively, with the hydrodynamic model and universal spectral forms for stratified and non-stratified turbulence and water temperature mixed by turbulence

proposed by Gibson (1980–1986) in a series of papers. Attempts are made to draw inferences about the possible hydrodynamic state of the fluid at the time of sampling, and more importantly, at previous times. The analysis leads to the conclusions that both composite spectra represent internal wave motions and temperature microstructure and fine structure that were produced by previous turbulence, but the microstructure fluid is non-turbulent at the time of sampling except at the smallest scales, and the turbulence and mixing processes have been vastly undersampled.

1.1. *The composite spectra*

Gargett *et al.* (1981) have combined measurements of the vertical gradient of horizontal velocity using three different instruments to produce a composite spectrum of vertical shear over a wide bandwidth from 10^{-2} to 50 c.p.m. The spectrum has a form similar to the schematic temperature gradient spectrum proposed by Gregg (1977), presumably because the physical processes which produce the shear and temperature-gradient fluctuations are closely related. Both data sets are from main thermocline layers at 28–38° N, with comparable mean Väisälä frequencies about 3 c.p.h. The two spectra are plotted with the same wavenumber k scale in figure 1 for comparison. Both have nearly constant level subranges at low wavenumbers, with transition to k^{-1} subranges at 0.07 and 0.08 c.p.m. and microstructure subranges beginning at 3 and 1 c.p.m. for the temperature and velocity spectra respectively. Gregg (1977) notes that the temperature microstructure spectral forms do not necessarily indicate high Reynolds number turbulence, and that the viscous–convective mixing process suggested by the k^{+1} subrange does not require the fluid to be turbulent, as pointed out by Batchelor (1959). However, Gregg (1980) concludes that the microstructure must be turbulent 'and not the decayed fossils of previous events' based on measurements of the separation distances between zero crossings of the temperature gradient and a timescale criterion. Gregg's criterion and conclusion are questioned by Gibson (1982*a*), and an alternative interpretation of the microstructure as fossil temperature turbulence is proposed.

Gargett *et al.* (1981) note the similarity between their microstructure bumps and the shape and ϵ dependence of the universal turbulence spectrum, and express the feeling that 'the spectral minimum at $\lambda = 2\pi(\epsilon/N^3)^{\frac{1}{2}}$ is the boundary between motions which are ... and aren't ... affected by the stratification of the ocean' (p. 1270). This conclusion that the full microstructure subrange represents turbulence unaffected by buoyancy is questioned in the present paper. Gargett *et al.* (1981) propose a universal buoyancy scaling hypothesis, based on the parameters ϵ and N, for the k^{-1} subrange which they consider to be saturated internal waves. In §3, this hypothesis is shown to be physically implausible and inconsistent with the observed k^{-1} form in the composite spectrum. The internal waves represented by the subrange are a factor of 14 lower than the saturated level predicted by the Gibson (1980–1986) theory.

1.2. *Hydrodynamic state and spectral forms*

According to universal similarity hypotheses of turbulence and turbulent mixing (Kolmogoroff 1941; Batchelor 1959; Gibson 1968), high-wavenumber spectra of all turbulent velocity and temperature fields should asymptotically approach universal forms when normalized by the appropriate length, time and temperature scales as the Reynolds number of the flow and range of turbulent scales in the cascade increases. Agreement with the expected universal spectral forms for one velocity component sampled in one direction, or for temperature sampled in one direction, does not prove that the fluid is turbulent. In principle, this proof would require an

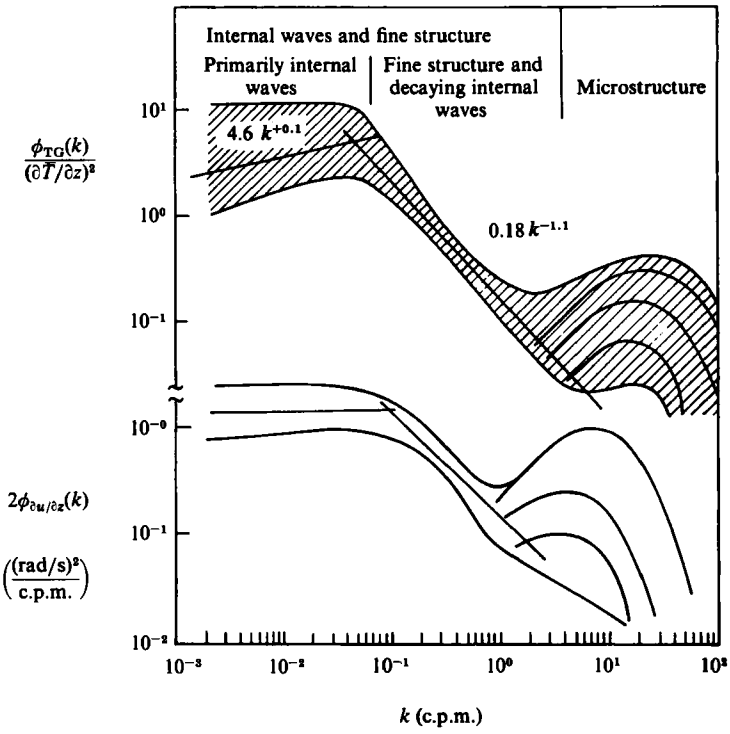

FIGURE 1. Schematic temperature-gradient spectrum of Gregg (1977) (upper) from 28 °N, 155 °W, 30–1200 m depth, compared to composite vertical-shear spectrum of Gargett *et al.* (1981) (lower) from 32–38 °N, 64–69 °W, 200–1500 m depth.

infinite number of statistical parameters of the observed flow (including spectra) sampled in all directions to agree with the expected isotropic universal forms. However, if a measured spectrum does *not* collapse to the universal form, or if the microstructure is quite anisotropic, the fluid cannot be turbulent, by hypothesis.

Turbulent flows are eddy-like motions where inertial forces dominate viscous and buoyancy forces over a finite range of lengthscales. The strongly diffusive nature of turbulence tends to homogenize the dissipation and strain rates within the turbulent region. Therefore, in making comparisons with universal forms or constants, statistical parameters must be normalized by dissipation rates averaged over scales within the turbulent range and within the turbulent fluid.

Universal forms are more powerful when used to identify non-turbulent rather than turbulent flows. Nature is notorious for producing frequency and wavenumber spectra with $-\frac{5}{3}$ power-law subranges in non-turbulent systems, as noted by Munk (1981). By the same token, the appearance of high-frequency bumps in oceanic shear and temperature gradient spectra may or may not signify the existence of turbulence.

From a profiling towed body, Schedvin (1979) finds that temperature-gradient spectra are often quite anisotropic even at the highest wavenumbers in an apparently turbulent microstructure bump. Such microstructure is non-turbulent at all scales since it is anisotropic at all scales. In some layers the observed microstructure spectra are isotropic with universal forms, but the forms indicate velocity dissipation rates ϵ so low that overturning turbulence would be impossible due to buoyancy forces of the ambient stratification based on the model of stratified turbulence and mixing

proposed by Gibson (1980). According to this model, the rate of strain of the microstructure fluid can be inferred by fitting the diffusive spectral cutoff to the Batchelor (1959) spectrum whether or not the microstructure is turbulent. The Batchelor lengthscale $L_B \equiv (D/\gamma)^{\frac{1}{2}}$ is inferred from the spectral fit, from which the rate of strain $\gamma = (\epsilon/\nu)^{\frac{1}{2}}$ can be computed, where D is the thermal diffusivity and ν is the kinematic viscosity. By assuming the critical Richardson number is $\frac{1}{4}$, Gibson (1980) derives the following criterion for existence of overturning turbulence in a stratified fluid,

$$\gamma \geqslant (5\text{–}6)\, N,$$

where N is the Väisälä frequency $[g(\partial\rho/\partial z)/\rho]^{\frac{1}{2}}$, g is gravity, ρ is density and z is depth. Stillinger (1981) and Stillinger, Helland & Van Atta (1983) find a similar criterion from stratified grid turbulence measurements; that is, vertically diffusive turbulence exists only when $\gamma \geqslant (4.9 \pm 0.1)N$. These measurements have recently been reproduced and extended by Itsweire, Helland & Van Atta (1986).

Gregg & Sanford (1980, 1981) question the validity of universal turbulent temperature-gradient spectra based on their measurements of temperature-gradient spectra from the MSR dropsonde in the mixed layer normalized using ϵ inferred from velocity-gradient spectra measured by Gargett more than 20 min later using the CAMEL dropsonde in the same depth range from a different ship. The universal scalar spectral form was observed, but with an enormous viscous–convective subrange constant $\beta_B = 57$ (later corrected to 20 in Gregg & Sanford 1981), much larger than the value of $\beta_B = 2$ suggested by Batchelor (1959) or the theoretically possible range of values $\sqrt{3} \leqslant \beta_B \leqslant 2\sqrt{3}$ derived by Gibson (1968). Numerous β_B values determined by careful laboratory and field studies are in the range 3 ± 1. Because the two dropsondes sampled water columns that were probably separated by a few hundred metres due to ship drift and surface currents, the strong possibility exists that ϵ for the two drops could differ by a factor of 100 if the dissipation rate in the layer is inhomogeneous or intermittent. This difference would resolve the discrepancy between the Gregg–Sanford measurements and universal similarity, and perhaps cast doubt on their assumption, often made in ocean microstructure studies, of horizontal homogeneity and a very large ratio of the horizontal to vertical scale of ocean turbulence patches. The idea is expressed by Gregg (1980) that 'turbulent patches are several meters thick and extend horizontally for up to a few kilometers', claiming such patches have been observed in the ocean from towed bodies. However, towed-body observations actually show that these 'patches' would be more aptly termed 'internal mixing layers'; that is, thin regions subjected to a common driving force with large horizontal extent, containing many individual turbulence patches with aspect ratios of order one, and with large horizontal intermittency, as observed by Schedvin (1979) and Washburn & Gibson (1984). The notion that oceanic turbulence patches are thin pancakes with homogeneous, non-intermittent internal ϵ and χ values is sometimes used to justify the dropsonde method of ocean turbulence sampling, and is quite erroneous.

Gargett (1985) also questions the validity of universal similarity for temperature spectra in water, based on measurements from a submarine in a tidal channel. Values of the scalar inertial subrange constant β_K up to 1.2 are reported that are double the generally accepted uncertainty range of 0.55 ± 0.05, with β_B values up to 12, which is 3–6 times larger than the expected range of 3 ± 1. These extreme values of β_K and β_B are interpreted by Gargett as evidence that 'the Corrsin–Oboukov–Batchelor (universal similarity) description is essentially incorrect as a description of the

spectrum of temperature fluctuations in water'. However, Gargett (1985) assumes the microstructure exhibiting the most extreme departures from universal similarity (with largest ϵ values) is unaffected by buoyancy, whereas most of it is classified in a mixed active-and-fossil-turbulence hydrodynamic regime according to the method of Gibson (1980), described in §2, with all but one of the classification parameter A_T values in the range 0.4–0.8 (see table 1 for the method and figure 2(*d*) for a plot of the Gargett A_T values). In this regime, strong departures from universal similarity are to be expected unless buoyancy effects are taken into account, particularly the strongly increased intermittency of dissipation rates in turbulent patches partially damped by buoyancy. Spectra are computed for records considerably larger than the maximum turbulent wavelength $\lambda = 1.2L_R$ proposed by Gibson (1981*a*), and the spectra are normalized by dissipation rates ϵ and χ averaged over total records covering 11–163 m rather than the local values. As mentioned previously, averaging together spectra from records larger than the local overturning scale (about $0.6L_R$) and from hydrodynamically different regions, and then normalizing these averaged spectra by non-locally averaged dissipation rates, may produce large, but spurious, departures from universal similarity forms and universal subrange constants. Gibson (1982*c*) extends the Batchelor (1959) theory to include microstructure in buoyancy dominated or other non-turbulent flows.

Gargett *et al.* (1981) infer a maximum overturning wavelength $\lambda_b = 2\pi(\epsilon/N^3)^{\frac{1}{2}}$ from their composite shear spectrum (p. 1267). This wavelength is larger by a factor of 5 than either the maximum overturning wavelength proposed by Gibson (1981*a*) or that measured by Stillinger (1981), both of which are in the range $(1.3 \pm 0.1)\ (\epsilon/N^3)^{\frac{1}{2}}$. The Gargett *et al.* (1981) wavelength represents the minimum wavenumber of the microstructure bump of their composite spectrum. No direct evidence is presented to show that the fluid was actually overturning at such large scales, with $\lambda = 1$–2 m. As shown in figure 1, the microstructure subrange of the Gregg (1977) composite temperature-gradient spectrum also begins at $\lambda = 1$–2 m, but by comparing nearly horizontal spectra from a thermistor mounted on a rotating wing and vertical spectra from the dropsonde nose, Gregg (1977) finds that the temperature microstructure was generally quite anisotropic and vertically stratified at wavelengths of 1–2 m. Therefore the fluid at this wavelength is not overturning and not turbulent. It seems likely that the Gargett *et al.* (1981) velocity microstructure bump is also not turbulent, especially at the larger wavelengths. From their table 1 (p. 1265), values of γ/N may be computed for three records 1*a* (200–400 m), 1*b* and 6 (400–600 m), giving $\gamma/N = 6.2$, 8.6 and 12.4, respectively. These values are very slightly larger than 5, the minimum required for turbulence by the Gibson (1980) and Stillinger (1981) criteria, indicating turbulence subranges of 0.09, 0.30 and 0.54 decades, compared to nearly 1.0 decades of microstructure subrange in the composite spectra which Gargett *et al.* (1981) interpret to be turbulence.

Gibson (1980) proposes that the large-scale fluctuations of most temperature and velocity microstructure measured in the ocean represents non-turbulent remnants of previous turbulent events, termed 'fossil turbulence'. Based on the decay of an isolated turbulent patch in a stratified fluid, the velocity and temperature gradient spectral forms for fossil turbulence are derived. In §2, a brief summary of the Gibson (1980, 1981*a*, *b*, 1982*a*–*c*, 1983, 1986) fossil turbulence model is given. In §3, the composite shear spectrum of Gargett *et al.* (1981) is compared to the Gibson (1980) fossil-vorticity-turbulence spectral forms. In §4, the Gregg (1977) composite temperature-gradient spectrum is compared to the Gibson (1980) fossil-temperature-turbulence spectral forms. Both comparisons suggest that the composite spectra

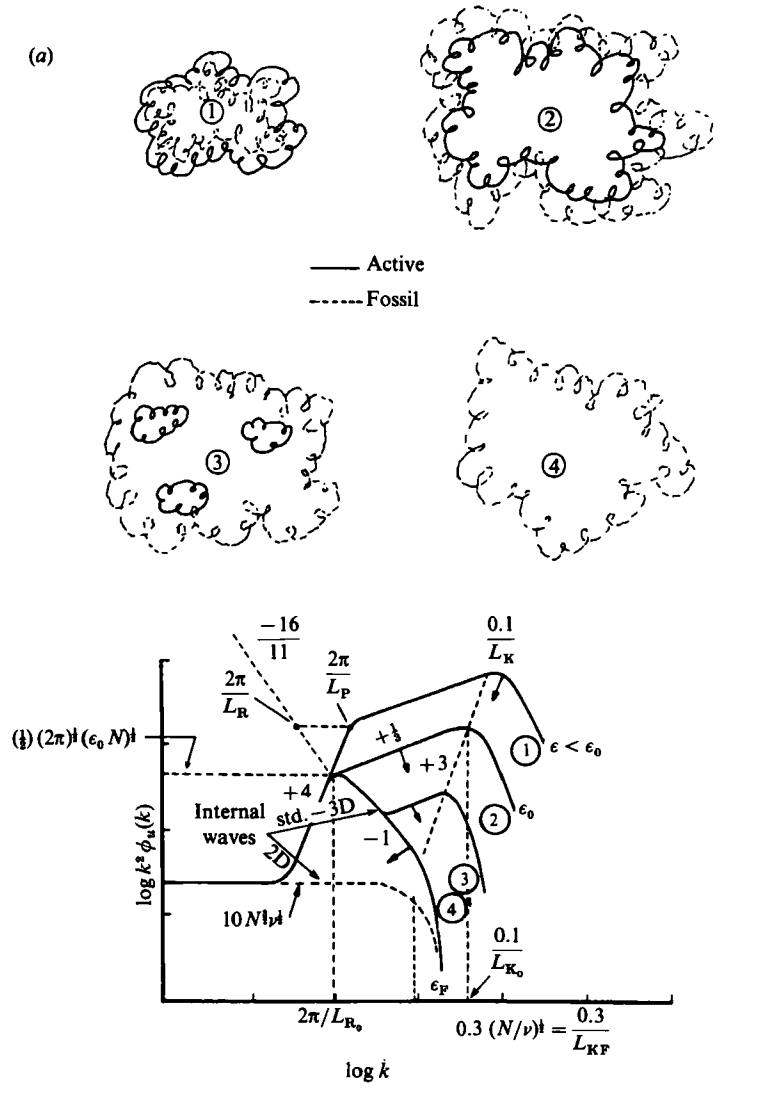

FIGURE 2(*a*, *b*). For caption see opposite page.

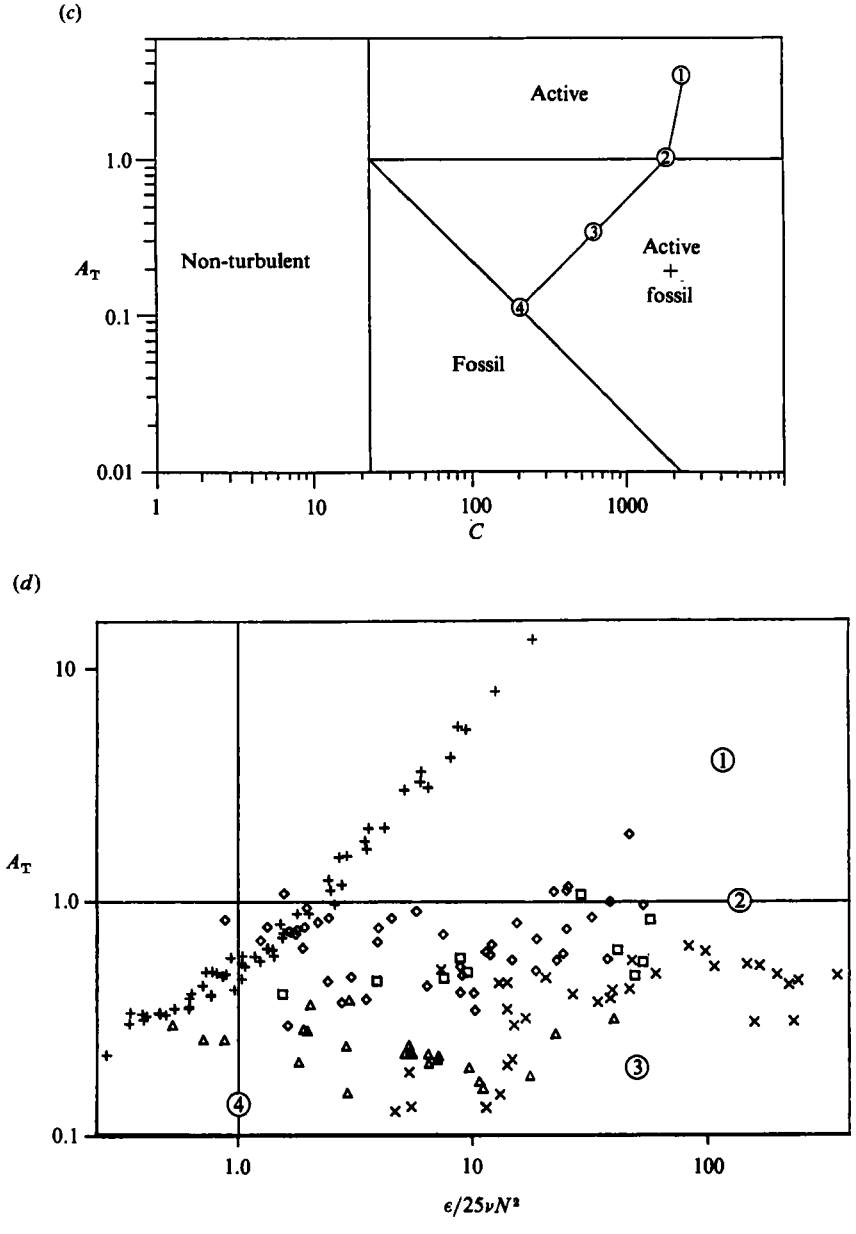

FIGURE 2. (*a*) Velocity-gradient spectra for a patch of active turbulence in a stably stratified medium after the source of turbulence is removed, from Gibson (1980). Stages of the patch evolution are shown schematically at the top. ① Active turbulence: $\epsilon > \epsilon_0$. ② Fossilization begins: $\epsilon = \epsilon_0$. ③ Transition: $\epsilon_0 > \epsilon > \epsilon_F$. ④ Fossil vorticity : turbulence: $\epsilon = \epsilon_F \sim 30\,\nu N^2$. (*b*) Temperature-gradient spectra corresponding to patch of active turbulence in region stratified by temperature. Same stages as in (*a*), from Gibson (1980). ① Actively turbulent temperature. ② Fossilization begins. ④ Fossil temperature turbulence. (*c*) Turbulence-activity parameter A_T versus Cox number C. The evolution of the fossilizing turbulence patch through the same stages as (*a*) and (*b*) is shown in this 'hydrodynamic phase diagram'. (*d*) Turbulence-activity parameter A_T *vs.* ϵ/ϵ_F. +, Laboratory stratified grid turbulence from Itsweire *et al.* (1986); ◇, Lake; ×, Ocean, low wind; △, Ocean, high wind from Dillon (1982); □, Knight Inlet from Gargett (1985). The four quadrants are active turbulence, active + fossil turbulence, fossil turbulence, and non-turbulent, for the upper right, lower-right, lower-left, and upper-left, respectively, in this 'hydrodynamic phase diagram'. The same hydrodynamic states 1–4 as in (*a*), (*b*) and (*c*) are shown.

represent fossil turbulence in the microstructure subranges and subsaturated (two–three)-dimensional internal waves in the k^{-1} fine-structure subranges.

The remaining notable feature of the composite spectra, the transition from a k^0 to a k^{-1} subrange at wavelengths of about 10 m, may also be a fossil remnant of previous turbulent activity. This corresponds to the beginning of the 'fine-structure' regime defined by Gregg in figure 1. The possibility is considered in §5 that the transition reflects the thickness of the average layer in a sheet and layer model, and that the layer thickness represents the largest overturning scale of previous turbulence patches. An attempt is made to quantify the degree of undersampling using an 'adequacy-of-sampling' parameter A_S.

Estimates of the maximum turbulent overturning scale in the deep ocean have tended to increase as the amount of data has increased and as more sensitive data analysis techniques have been employed. Gregg (1977) at first reported that 'in mid-gyre, overturns with vertical scales of 1 m are not common. Although weakly stratified regions several meters thick have been found *there is no evidence* that they were produced by overturns with correspondingly greater scales' (italics added). However, just such strong evidence of large overturns was later discovered by Gregg (1980) in subsequent analysis of the same data: Thorpe overturning scales (vertical displacements required to produce a monotonic temperature profile) within several of the weakly stratified layers are found to be nearly as large as the layer thicknesses, with maximum value of 7.5 metres in a 10 m thick 'isothermal' layer. Many of the layers including the thickest one, are embedded in surrounding fluid which is stable to double diffusive mixing.

Other mechanisms besides turbulence may determine layer thicknesses, particularly double diffusive or 'salt-fingering' instabilities. However, it appears that turbulence may be the dominant mechanism in at least some regions, such as the main thermocline in the Pacific, where double diffusive mixing may be relatively weak.

1.3. *Hydropaleontology of oceanic microstructure*

Because many patches of microstructure activity are included in data sets such as Gregg (1977) or Oakey & Elliott (1980), it is reasonable to assume that record averages are representative of the turbulence process if it is assumed that the patches are turbulent. However, comparison with the fossil-turbulence model of Gibson (1980–1986) indicates that none of the patches are actively turbulent at the largest scales and many patches are non-turbulent at all scales. Furthermore, the larger patches, which represent the most effective mixing regions, are usually in the most advanced state of decay, presumably because their life expectancy is greater than patches formed by weaker turbulence.

Assuming that all microstructure patches are actively turbulent when they are actually fossils can be quite misleading. Gregg (1977) estimates a vertical diffusivity about 10^{-2} less than values estimated from bulk properties of the main thermocline in the Pacific Gyre, and Oakey & Elliott (1980) estimate a vertical heat flux 10^{-2} less than an estimate from bulk properties of the Denmark Strait overflow boundary. Neither data set includes large microstructure patches which are actively turbulent at the largest scales. Temperature microstructure with wavelengths up to 10 m is observed, but the maximum active turbulence wavelengths are less than a metre. Gibson (1982*a*, *b*) shows that even the large overturning scale patches of Gregg (1977, 1980) and the very-high-Cox-number microstructure patches of Oakey & Elliott (1980) are fossil temperature turbulence in an advanced state of decay, with dissipation rates 3–5 orders of magnitude less at the time of observation than when

the patches were actively turbulent. Gibson (1981*b*) proposes that actively turbulent patches, which dominate the vertical diffusion process in many ocean regions, may have been severely undersampled, leading to large underestimates of space–time average dissipation rates and vertical diffusivities.

Recognizing that the observed microstructure is fossil turbulence resolves the discrepancy between the microstructure and bulk-flow estimates of vertical diffusivity in a rather unsatisfactory way: all that can be concluded is that the microstructure diffusivity and mean dissipation estimates are lower bounds to the true values. The 'hydropaleontology' of fossil turbulence modelling has not progressed to a stage that permits reliable estimates of space–time average turbulence properties by extrapolation from a small number of microstructure measurements. Until this occurs, the only option is to collect such large data sets that the biggest and strongest microstructure patches, the 'big bangs' which apparently dominate the turbulent mixing and diffusion processes in the ocean, are included in their fully turbulent state.

2. The fossil-turbulence model of Gibson (1980–86)

The basic ideas and evidence for fossil turbulence in the ocean and atmosphere have been in print for over fifteen years, starting with Woods *et al.* (1969) and Nasmyth (1970). However, little mention of the phenomenon has appeared since, other than the Gibson (1980–86) papers and denials of its existence in various data sets, for example Caldwell *et al.* (1980), Dillon & Caldwell (1980), Gregg (1980), Gregg & Sanford (1980), Dillon (1982), Crawford (1982), Caldwell (1983), Dillon (1984) and Gregg (1984). Such denials are often based on a definition of fossil turbulence, introduced by Nasmyth (1970), which is not physically possible; that is, isotropic fluctuations of temperature (density) caused by turbulence which persist after the velocity field has decayed to zero. All isotropic density microstructure fields subjected to gravitational acceleration must contain density inversions and must therefore contain velocity fluctuations. However, it is not necessary that these velocity fluctuations be *turbulent*, as assumed by Gregg (1980). Gibson (1982*a*) shows that restratification motions of fossil temperature turbulence microstructure, in which density inversions will always exist, are stabilized by both viscosity and thermal diffusion, and may be non-turbulent. Neither is it true that $\epsilon \geqslant 25\nu N^2$ is an indication that microstructure is not fossilized, as assumed by Gregg (1984), since the largest scales may be fossil even though the small scales are active.

A dynamical model of the fossil-turbulence process and a comparison with available oceanographic microstructure measurements is given in the sequence of papers Gibson (1980–1981*a*, *b*, 1982*a–c*, 1983, 1986). The collection is referred to in this paper as the Gibson (1980–86) fossil-turbulence model.

Gibson (1980) considers the evolution of an isolated patch of actively turbulent fluid embedded in a stably stratified region of non-turbulent fluid, shown schematically at the top of figure 2(*a*). Density variations are assumed to be entirely due to variations in temperature, and the fluid is assumed to be water, for simplicity. Spectral forms for the velocity field and scalar field at various stages of the evolution are shown in figures 2(*a*) and (*b*). At stage 1 the patch has lengthscale L_{P} and the velocity-gradient spectrum in figure 2(*a*) and the temperature-gradient spectrum in figure 2(*b*) should be the universal forms for non-stratified turbulence and for turbulent mixing of high-Prandtl-number passive scalars respectively.

As the patch grows by entraining ambient fluid the velocity-gradient spectral level falls and the range of turbulent scales narrows. The wavelength range of turbulent

temperature fluctuations also narrows, but the level of the spectrum rises because the temperature difference between fluid entrained at the top and bottom increases as the patch grows.

At stage 2 fossilization begins; that is, the inertial forces of the largest turbulent eddies in the patch become equal to the buoyancy forces of the surrounding stably stratified medium. This occurs when the patch size L_P becomes approximately equal to the buoyancy scale $L_R \equiv (\epsilon/N^3)^{\frac{1}{2}}$. In figure 2(*a*) the point of fossilization occurs when the locus of points marking the largest eddies in the patch, with slope +4, intersects the locus of points marking the buoyancy wavenumber at the same spectral level, with slope $-\frac{16}{11}$. The actual wavelength of the intersection is estimated by Gibson (1981*a*) to be $\lambda = 1.2L_R$, slightly larger than the estimate of $\lambda = L_R$ shown in figure 2(*a*), from Gibson (1980).

Setting the scalar inertial subrange equal to the most active 'fine structure' subrange observed by Gregg (1977) at the fossilization wavelength L_{R_0} gives

$$\epsilon_0 \approx 13DC_0N^2, \tag{1}$$

which Gibson (1980) proposes as a criterion for discriminating between hydrodynamic states of stratified microstructure. Microstructure with ϵ greater than $13DCN^2$ is classified as active turbulence. Equality indicates active turbulence at fossilization. Values of ϵ less than $13DCN^2$ indicate fossil turbulence for $L_P > \lambda > L_R$ and active turbulence for $L_R > \lambda > 0.1L_K$. A turbulence activity parameter A_T is defined in Gibson (1980)

$$A_T \equiv \left(\frac{\epsilon}{13DCN^2}\right)^{\frac{1}{2}}, \tag{2a}$$

in order to classify the hydrodynamic state of stratified microstructure, as shown in table 1.

Value of A_T	Hydrodynamic state of microstructure
$A_T > 1$	Active turbulence
$A_T = 1$	Turbulence at fossilization
$1 > A_T > A_F$	Mixed active and fossil turbulence
$A_T = A_F$	Completely fossil turbulence
$A_T < A_F$	Decayed fossil turbulence
$1 < A_T < (\epsilon_F/\epsilon)\,A_T$	Non-turbulence

$A_T \equiv (\epsilon/13DCN^2)^{\frac{1}{2}}$
$A_F \equiv (\epsilon_F/13DCN^2)^{\frac{1}{2}}$
$\epsilon_F \equiv 24.5\nu N^2$

TABLE 1. Turbulence activity parameter A_T

where ϵ and C are measured within the microstructure patch and N is averaged over the immediately surrounding vertical water column. The value of A_T at complete fossilization is

$$A_T = A_F = 1.4\left(\frac{Pr}{C}\right)^{\frac{1}{2}}, \tag{2b}$$

from the definitions of A_F and ϵ_F in table 1.

An equivalent method of classifying the hydrodynamic state of stratified microstructure is to plot boundaries separating the various hydrodynamic states for A_T versus C, as shown in figure 2(*c*). This forms a hydrodynamic phase diagram $A_T(C)$,

which is divided into various hydrodynamic regimes according to the criteria given in table 1. Several equivalent hydrodynamic phase diagrams $A_T^0(x)$ are used in Gibson (1980–86) to classify oceanic microstructure data sets, where

$$A_T^0(x) \equiv \left[\frac{\epsilon}{\epsilon_0(x)}\right]^{\frac{1}{2}}, \tag{2c}$$

and x is any parameter of the microstructure from which the dissipation rate at fossilization $\epsilon_0(x)$ can be estimated; for example, the maximum Thorpe overturning scale L_T.

The evolution of $A_T(C)$ for the microstructure patch of figure 2(*a*, *b*) is shown in figure 2(*c*). In the 'active-turbulence' regime the locus has slope +5 and in the 'mixed active+fossil-turbulence' regime the locus has slope +1, from the definition of A_T and the ϵ dependence of C for these two regimes given in the Gibson (1980) model. According to the model, $C \sim \epsilon^{\frac{1}{11}}$ for active turbulence, and $C \sim \epsilon^{\frac{1}{3}}$ in the mixed-active+fossil regime, giving the indicated power laws. Most oceanic and lake microstructure patches have A_T values in the active-fossil regime, with $1 > A_T > 0.01$ and $C_{tr} \approx 2Pr < C < 10^5$, where the transition Cox number C_{tr} of about 20 for temperature in water is shown in figure 2(*c*). Caldwell *et al.* (1980) propose a scaling law for oceanic turbulence based on their observation that A_T values have a mean value near 0.25 for upper ocean patches.

Figure 2(*d*) is an alternative form of the hydrodynamic phase diagram in figure 2(*c*). Values of A_T for laboratory, lake and ocean, and Knight Inlet data sets are plotted versus the ratio ϵ/ϵ_F, from Itsweire *et al.* (1986), Dillon (1982) and Gargett (1985) respectively. The stratified grid turbulence values progress from the actively-turbulent quadrant in the upper right of figure 2(*d*), through the mixed active-and-fossil turbulence quadrant in the lower right, and into the decayed-fossil regime in the lower left as the fluid leaves the test section. Naturally occurring stratified microstructure is rarely found outside the mixed active-and-fossil regime. Because the formation processes, such as breaking internal waves, generally include buoyancy forces, most natural stratified turbulence events originate along the horizontal line in figure 2(*d*), corresponding to turbulence at fossilization, and not in the completely active regime. Because the fossil microstructure patches are bounded by large-density-gradient surfaces on which parasitic secondary turbulence patches may form, the microstructure $A_T(\epsilon/\epsilon_F)$ values tend to stay to the right of the vertical line, and do not become completely fossil. As shown in figure 2(*d*), naturally occurring stratified turbulent patches have much larger ϵ/ϵ_F values, corresponding to higher Reynolds numbers, than observed in the laboratory study. The lake values are from near the surface during wind forcing, and tend to have A_T values near 1.0. The Knight Inlet values were not measured at the turbulence generation site (a shallow sill) for safety reasons, and are mostly in the mixed active-and-fossil regime. The ocean values are from patches at depths 10–50 m in the mixed layer and seasonal thermocline, and are always fossil at the largest scales, indicating undersampling.

The quantity $B_0 \equiv (\epsilon/DCN^2)_0$ at fossilization is a crucially important universal constant of stratified turbulence. By estimating C_{tr} from ocean and lake data of Dillon (1982) and from a theoretical model, Gibson (1986) confirms the value of about 13 proposed by Gibson (1980). Determination of a more precise value by appropriate laboratory or computer modelling is a subject of current research. Itsweire *et al.* (1986) find B_0 values of about 4–7 in stratified grid turbulence. This is significantly less than the value of 13 ± 3 estimated for isolated patches by Gibson (1980, 1986), much larger than the (constant) value of 0.8 inferred from oceanic measurements by Caldwell

et al. (1980) but in agreement with the value of 4 proposed by Dillon (1984). Most of the discrepancy between the B_0 values of Gibson (1980, 1986), ≈ 13, and the Dillon (1984) value, ≈ 4, can be attributed to their different methods of estimating $\partial\bar{\rho}/\partial z \sim B_0$. The former is based on the (larger) external mean gradient and the latter on an internal mean gradient formed by reordering the density fluctuations within the patch into a monotonic profile. Similarly, the grid-turbulence estimates of mean density gradients may be smaller than appropriate for isolated patches, and therefore may give smaller estimates of B_0. The Caldwell *et al.* (1980) value of 0.8 is presumably small because the microstructure is fossil.

Using a larger grid, Itsweire *et al.* (1986) extend and confirm the Stillinger *et al.* (1983) results, and report a stratified turbulence criterion of $\gamma \geqslant (4\text{–}5)\,N$, close to the Gibson (1980) and Stillinger *et al.* (1983) criteria.

Stage 3 in figure 2 (*a*) is in transition between fossilization and complete fossilization. The viscous dissipation rate ϵ is intermediate between ϵ_0 and ϵ_F, where

$$\epsilon_F \approx 30\,\nu N^2, \tag{3}$$

according to Gibson (1980) based on a buoyant–inertial–viscous transition Richardson number $N^2/[\partial u/\partial z]^2 = \frac{1}{4}$, using the isotropic relation $\epsilon \approx [\frac{15}{2}][\partial u/\partial z]^2$ at this transition. This estimate has been confirmed by Stillinger (1981) (also reported in Stillinger *et al.* 1983), who finds

$$\epsilon_F = 24.5\,\nu N^2, \tag{4}$$

by direct measurements in stratified grid turbulence.

The velocity-gradient spectrum in transition consists of two subranges: the 'fossil vorticity turbulence' or 'saturated three-dimensional internal wave' subrange

$$\phi_{[\partial u/\partial z]} = 6.7\,N^2 k^{-1}, \tag{5}$$

which is the locus of points marking the beginning of the inertial subrange of the turbulent velocity spectrum, setting the wavelength $\lambda = 1.2L_R$. The constant $c = 6.7$ is $(\frac{4}{3})\alpha(2\pi/1.2)^{\frac{4}{3}}$, taking the universal inertial subrange constant $\alpha = 0.55$. A slightly smaller value of the constant, $c = 5.8$, was given in Gibson (1980, 1981*a*). The constant and its uncertainty range is about 6.7 ± 1.8. As the embedded turbulence within the patch decays, the turbulent kinetic energy of the largest overturning eddies will be converted to buoyancy dominated bobbing motions (internal waves) with the same spectral level and wavelength as the eddies. Because their bobbing frequency is N, these saturated waves have nearly zero propagation velocity and will remain within or near the patch and their spectrum will retain its form. The dissipation rate ϵ within the patch draws energy from the embedded turbulence whose maximum overturning wavelength $1.2L_R$ decreases as ϵ decreases and is smaller than $1.2L_{R_0}$ because ϵ is smaller than ϵ_0. The 'active turbulence' subrange has universal form with decreasing range of scales as ϵ decreases. Ultimately the buoyancy scale converges to the viscous scale and all 'active' or 'overturning' turbulence disappears, leaving only the remnant 'fossil-vorticity-turbulence' spectrum, shown as stage 4 in figure 2 (*a*).

A particular lengthscale for the velocity field emerges from the analysis at the buoyant–inertial–viscous (BIV) transition point, with $\epsilon \approx 30\,\nu N^2$, denoted by Gibson (1980) as the 'fossil Kolmogoroff scale' $L_{KF} \equiv (\nu/N)^{\frac{1}{2}}$. A corresponding 'fossil Batchelor scale' $L_{BF} \equiv (D/N)^{\frac{1}{2}}$ represents the microscale of the temperature fluctuations at the BIV transition point. The wavelength of overturning eddies at this unique hydrodynamic state of stratified flow is estimated by Gibson (1981*a*) to be

$\lambda = 6.1 L_{\mathrm{KF}}$. Detailed modelling of the BIV transition is given in Gibson (1986) which shows that

$$C_{\mathrm{tr}} = C_{\mathrm{BIV}} \approx 2Pr \tag{6}$$

so that the constant $B_0 \approx 13$ by setting $\epsilon_{\mathrm{tr}} = 30\,\nu N^2$.

Kinetic energy decay in the completely fossil-turbulence patch is much slower than it was in the actively turbulent state. Because the kinetic energy KE in the fossil patch is approximately the same as in the active patch at fossilization (stage 2), the decay period $\tau_\omega \approx \mathrm{KE}/\epsilon$ will be approximately the buoyancy period N^{-1}, the decay period of the active patch at fossilization, times the ratio $\epsilon_0/\epsilon_{\mathrm{F}}$. In terms of the patch size

$$\tau_\omega \approx N^{-1}(L_{\mathrm{R}_0}/L_{\mathrm{KF}})^2 \approx N^{-1} Re_0^{\frac{3}{2}}, \tag{7}$$

which shows that large fossil-vorticity-turbulence patches, produced by turbulence with large Reynolds numbers at fossilization Re_0, last longer than small ones.

The constant spectral level $10 N^{\frac{3}{2}} \nu^{\frac{1}{2}}$ represents a limiting case of a stratified non-turbulent viscous fluid with nearly horizontal two-dimensional internal waves at transition, discussed by Gibson (1980). The straining motions may create density gradient and vorticity layer sheets with maximum rate-of-strain $\gamma_{\mathrm{F}} \approx 5N$ and corresponding minimum viscous-boundary-layer thickness $\approx 3L_{\mathrm{KF}}$ without transition to turbulence. The thermal-boundary-layer thickness on the sheets will be $\approx 3L_{\mathrm{KB}}$. If the sheets are separated by a layer thickness L_{L}, and if the vorticity concentrates on the sheets with saturated rate-of-strain γ_{F}, the vertical shear spectrum should be white with level $\approx 10(L_{\mathrm{L}}/L_{\mathrm{KF}}) N^{\frac{3}{2}} \nu^{\frac{1}{2}}$ for wavelengths larger than $\lambda_{\mathrm{L}} \approx 2L_{\mathrm{L}}$, and with a saturated k^{-1} subrange corresponding to the universal fossil-vorticity-turbulence spectrum shown as stage 4 in figure 2(*a*). If $\gamma < \gamma_{\mathrm{F}}$ on the sheets, a fine-structure spectrum

$$\phi_{[\partial u/\partial z]} = cN^2 k^{-1}, \tag{8}$$

should still be observed from vertical profiles for $L_{\mathrm{L}} > \lambda > 6L_{\mathrm{KF}}$, but the constant c will be less than the saturated value of 6.7. Further discussion is given in §3.

The peak of the temperature-gradient spectrum in the active phase of the patch increases along a locus with slope $-\frac{7}{11}$, as shown in figure 2(*b*). The beginning of the scalar inertial subrange (slope $+\frac{1}{3}$) has a locus of slope -1, and also increases in level as the wavenumber range of the subrange decreases. The universal spectral form for a turbulent scalar field with Prandtl number ν/D about 10 should be preserved for the full range of turbulent scales as L_{P} grows toward the buoyancy scale at fossilization L_{R_0} (stage 2 in figure 2*b*).

During the fossilization phase of the patch evolution, the viscous–convective subrange should preserve its form but shift from a peak at the Batchelor scale L_{B} to the fossil Batchelor scale L_{BF}, shown as stage 4 in figure 2(*b*). The lower wavenumber portion of the scalar gradient spectrum should be relatively unaffected by the fossilization process, according to the Gibson (1980) model.

From figure 2(*b*) it is clear that the scalar dissipation rate after fossilization of the patch (stage 4) is not much different to that before (stage 2). Therefore the decay time of fossil temperature turbulence is less than that for fossil vorticity turbulence. According to Gibson (1980) the decay time is

$$\tau_{\mathrm{T}} = (\gamma_0/N)^{\frac{2}{3}} N^{-1}, \tag{9}$$

compared with

$$\tau_\omega = (\gamma_0/N)^2 N^{-1}, \tag{10}$$

for fossil vorticity turbulence.

The term 'persistence time' used by Gibson (1980) for the preceding τ quantities is somewhat misleading, and is replaced by 'dissipation time scale' in Gibson (1981*a*).

The persistence time, or period of detectability Θ, of a turbulence fossil will depend on many factors, but will generally be much longer than the τ values given above. Because internal-wave energy can radiate away from the fossil patch and temperature fluctuations can only disappear by molecular diffusion, it seems likely that $\Theta_T \gg \Theta_\omega$, contrary to the ordering indicated by (9) and (10), where $\tau_\omega \gg \tau_T$.

Some other minor changes in the Gibson (1980) fossil-turbulence model are suggested in the series of papers Gibson (1981*a*, *b*, 1982*a–c*, 1983, 1986), along with comparisons to available microstructure data sets. A wavelength criterion for the existence of stratified turbulence is proposed in Gibson (1981*a*) based on (4) and the form of the universal turbulent-velocity spectrum, to give

$$1.2L_R \geqslant \lambda \geqslant 15L_K, \tag{11}$$

where λ is the wavelength of a turbulent Fourier element. Use of a modified turbulence activity parameter A_T^0 based on C_0 rather than C is discussed. The model is extended in Gibson (1986) to account for the erosion of the upper and lower boundaries of decayed fossil patches of primary turbulence events by secondary turbulence events which tend to form at these sheets of sharp vertical density gradient. Gibson (1981*b*, 1982*a–c*, 1983) compare the model with various oceanic data sets and alternative hydrodynamic interpretations.

The locus of points marking the beginning of the scalar inertial subrange is used by Gibson (1982*a*) to derive the form of the saturated internal wave temperature gradient spectrum

$$\phi_{[\partial T/\partial z]} = 0.7\left(\frac{\partial \bar{T}}{\partial z}\right)^2 k^{-1}, \tag{12}$$

which is in good agreement with the same equation proposed by Gibson (1980) with a proportionality constant $d = 0.9$, rather than 0.7, inferred from the Gregg (1977) data. Further discussion is given in §4.

3. The composite vertical-shear spectrum of Gargett *et al.* (1981) compared to the spectral theory of Gibson (1980)

In order to determine whether the microstructure subrange of the composite shear spectrum represents turbulent or non-turbulent fluid, we may compare the spectral forms with the universal form; for example, the form determined empirically by Gibson & Schwarz (1963) from grid turbulence measurements and the tidal channel measurements of Grant, Stewart & Moilliet (1962), or the wake, jet and atmospheric boundary-layer measurements of Champagne (1978). Agreement with the universal spectral form is a necessary but not sufficient condition for the fluid to be turbulent, as mentioned in §1.

By turbulence we mean the three-dimensional, eddy-like state of fluid motion which arises when inertial forces dominate buoyancy and viscous forces which tend to damp out the eddies, as discussed by Gibson (1980, 1981*a*) and mentioned above. This is a narrow definition, which includes the class of fluid motions which produces most of the irreversible mixing, and excludes motions dominated by buoyancy which are considered to be internal waves. Definitions of 'turbulence' are available which are so broad that nearly any random fluid process is included, for example, Lanford (1982). However, such definitions are of little utility in describing mixing and diffusional processes in the ocean, where buoyancy-dominated flows are remarkably less effective than turbulence in producing irreversible mixing. Gargett *et al.* (1981) assume buoyancy forces must be negligible in the motions which they classify as turbulent, so their definition of turbulence coincides with that used in this paper.

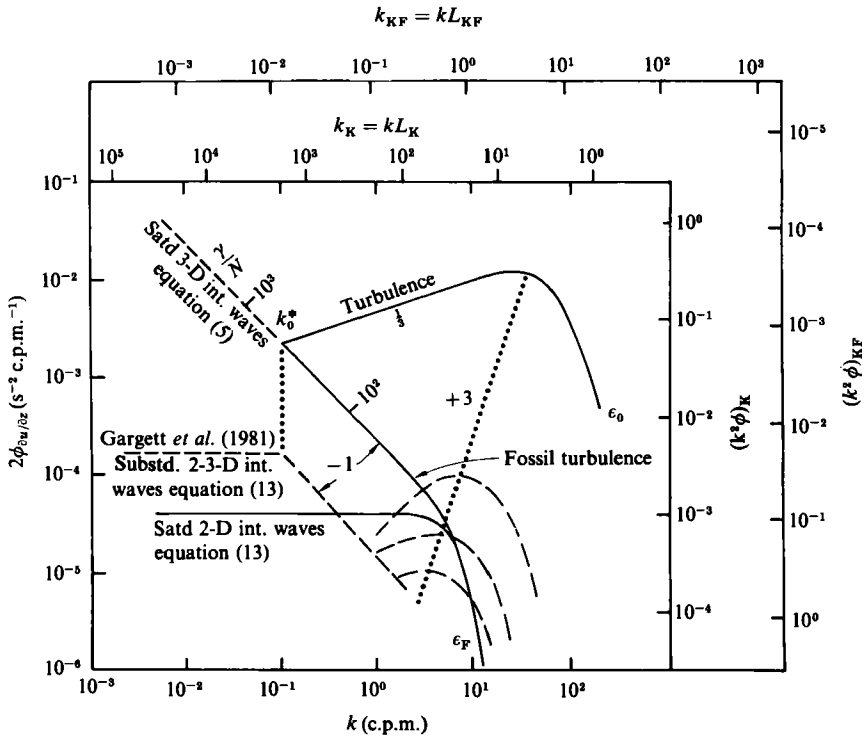

FIGURE 3. Composite vertical-shear spectrum of Gargett *et al.* (1981) compared with universal stratified-turbulence spectra of Gibson (1980). Because the k^{-1} subrange of the composite spectrum is below the universal three-dimensional saturated internal wave spectrum of (5), the motions are interpreted as (two–three)-dimensional subsaturated internal waves. The microstructure subrange appears to be essentially non-turbulent fossil vorticity turbulence. A turbulence spectrum is shown corresponding to the dissipation rate $\epsilon_0 = 0.044$ cm^2/s^3 indicated by the transition wavenumber $k_0 = 0.1$ c.p.m. assuming this represents the mixed-layer thickness of turbulence in the ocean interior. Kolmogoroff (1941) turbulence scaling and Gibson (1980) fossil-turbulence scaling of the spectra are shown at the right and top.

Figure 3 shows a comparison of the Gargett *et al.* (1981) shear spectrum with the Gibson (1980) spectrum discussed in §2 and shown in figure 2(*a*).

The k^{-1} subrange of the composite spectrum is compared with the saturated internal-wave spectrum by computing c from (8) for the composite spectrum and comparing this value with the saturated value of 6.7, from (5). Substituting $\phi_{[\partial u/\partial z]} = \frac{1}{2}\phi_S = (1.5/2) \times 10^{-5}$ s^{-2}/c.p.m. at $k = 1$ c.p.m. and $N = 4 \times 10^{-3}$ rad/s (2.3 c.p.h.) gives $c = 0.47$, which is less than 6.7 by a factor of 14.3. Therefore the composite k^{-1} spectrum of Gargett *et al.* (1980) is strongly subsaturated.

Figure 3 shows the composite shear spectrum compared with the saturated three-dimensional internal wave spectrum of (5), with viscous cutoff at $k = (N/\nu)^{\frac{1}{2}}$, corresponding to the saturated fossil-vorticity-turbulence spectrum of Gibson (1980). The k^{-1} portion of the composite spectrum is 14.3 times less than the saturated level, and only a small portion of the microstructure range is above the saturated line indicating a short range of possible turbulence. The microstructure peaks follow the universal locus of turbulence spectral peaks, with slope +3. The dissipation rate ϵ_F of the fossil-vorticity-turbulence spectrum is $\nu(5N)^2 = 4.8 \times 10^{-6}$ cm^2/s^2, comparable with the measured values of Gargett *et al.* (1981). As mentioned previously, the range

of turbulent wavelengths indicated is between 0.09 and 0.5 decades, much smaller than the 1.0 decade range of turbulence inferred by Gargett *et al.* (1981).

Also shown in figure 3 is a universal active-turbulence spectrum with dissipation rate ϵ_0 corresponding to the assumption that the transition wavenumber $k_0 = 10^{-1}$ c.p.m. $= k_0^*$ is a fossil remnant of previous turbulence with overturning wavelength $\lambda_0 = k_0^{-1} = 1.2(\epsilon_0/N^3)^{\frac{1}{2}}$. Inspection of the measured temperature profiles shows the usual smoothed step-like profile, with step thicknesses of 3–10 m, which is consistent with the hypothesis that k_0 reflects the mean quasi-mixed-layer thickness.

However, the ϵ_0 value computed from k_0 and N is 4.4×10^{-2} cm^2/s^3. This is very large compared with the composite microstructure values, which are in the range $(7\text{–}39) \times 10^{-6}$ cm^2/s^3. If the layers represent previously turbulent mixed layers, then the mixing process must be very patchy in space and intermittent in time. For example, if the average ϵ were 10^{-5} cm^2/s^3, then the volume fraction of space–time occupied by turbulence would be 2.2×10^{-4}. In order to expect to see such an event, about 45 km of vertical profile record are required if the process is stationary in time and the active patches are not clustered together in either space or time (as they actually seem to be). This is about 50 times more data than was used in preparing the microstructure portion of the composite shear spectrum.

Gregg (1980) detected nearly isothermal patches of microstructure in the main thermocline with Thorpe overturning scales as large as 3–7.5 m and vertical thickness up to 10 m, so the turbulence mechanism of producing mixed layers in the ocean interior apparently exists. Whether turbulence produces most of the 'fine structure' represented by the k^0–k^{-1} transition of the composite spectra of figure 1, or whether the steps are due to large-scale internal wave straining, double diffusive mixing, or some combination of all three mechanisms remains as an interesting challenge for future studies.

Figure 3 also shows the spectral axes normalized using both Kolmogoroff scaling and the buoyancy scaling proposed by Gibson (1980) (see table 2, §4). Kolmogoroff scaling is accomplished by means of the Kolmogoroff length $L_{\mathrm{K}} = (\nu^3/\epsilon)^{\frac{1}{4}}$ and Kolmogoroff time $T_{\mathrm{K}} = (\nu/\epsilon)^{\frac{1}{2}}$. Buoyancy scaling of Gibson (1980) is based on viscous–buoyancy (fossil Kolmogoroff) length- and timescales $L_{\mathrm{KF}} = (\nu/N)^{\frac{1}{2}}$ and $T_{\mathrm{KF}} = N^{-1}$, respectively. Since the velocity-gradient spectrum has units $T^{-2}L$, then $(k^2\phi)_{\mathrm{K}} = (k^2\phi)\, T_{\mathrm{K}}^2\, L_{\mathrm{K}}^{-1}$ and $(k^2\phi)_{\mathrm{KF}} = (k^2\phi)\, T_{\mathrm{KF}}^2\, L_{\mathrm{KF}}^{-1}$. These are shown as the right-hand ordinates of figure 3. Correspondingly, $k_{\mathrm{K}} = kL_{\mathrm{K}}$ and $k_{\mathrm{KF}} = kL_{\mathrm{KF}}$ abscissas are shown at the top.

The Gibson (1980) buoyancy scaling for saturated internal waves is based on two universal similarity hypotheses analogous to those proposed by Kolmogoroff (1941) to describe the statistical laws of high-Reynolds-number turbulence. It is assumed that a fluid of viscosity ν is stably stratified with uniform N, and that homogeneous, nearly isotropic motions are excited to the maximum amplitude which can possibly exist without becoming turbulent.

First similarity hypothesis for saturated internal waves

The first similarity hypothesis for saturated internal waves is that the probability laws of velocity differences for points separated by distances $y < L_{\mathrm{L}}$ should become universally similar when normalized by the lengthscale $L_{\mathrm{KF}} = (\nu/N)^{\frac{1}{2}}$ and timescale $T_{\mathrm{KF}} = N^{-1}$, where L_{L} represents the largest saturated internal-wave motion.

The first similarity hypothesis of saturated internal waves is much like the Kolmogoroff (1941) first similarity hypothesis of turbulence, except that both the local Reynolds number $L_{KF}^2/\nu T_{KF}$ and the local Richardson number $N^2/(L_{KF}/T_{KF}\,L_{KF})^2$ must be at critical values of order 1. Recall that for turbulence, only the local Reynolds number $L_K^2/\nu T_K$ must be at a critical value of order 1.

Second similarity hypothesis of saturated internal waves

The second similarity hypothesis of saturated internal waves is that for points separated by distances much larger than $L_{KF} = (\nu/N)^{\frac{1}{2}}$ but less than L_L, the probability laws for velocity differences should be independent of viscosity.

According to the second hypothesis the shear spectrum $k^2\phi_u$ should depend only on k and N for $L_L^{-1} < k < L_{KF}^{-1}$. Therefore, by dimensional analysis we find that $k^2\phi_u = cN^2k^{-1}$, where c is a universal constant, reproducing (8). The analogy to the second similarity hypothesis of Kolmogoroff (1941) is apparent: by that hypothesis turbulent motions on scales larger than L_K should be independent of viscosity and dependent only on ϵ and k. By dimensional analysis the spectrum $k^2\phi_u = \alpha\epsilon^{\frac{2}{3}}k^{\frac{1}{3}}$, the turbulent inertial subrange, where α is a universal constant.

Buoyancy scaling hypothesis of Gargett et al. (1981)

A different buoyancy scaling is proposed by Gargett *et al.* (1981) based on the assumption that saturated nonlinear internal-wave motions, termed 'buoyancy-modified turbulence or turbulence-modified waves', will depend on both N and ϵ for $L_L^{-1} < k < L_R^{-1}$ giving a lengthscale $L_R = (\epsilon/N^3)^{\frac{1}{2}}$ and timescale N^{-1}. This assumption is physically implausible since it requires that the spectral level of saturated internal wave motions depend on the dissipation rate ϵ of the embedded turbulence which is on much smaller scales than the saturated wave motions. The assumption is contrary to the Miles–Howard criterion (Miles 1961; Howard 1961) for the stability of stratified shear flows, which suggests that instability will occur at a critical Richardson number $Ri = N^2/(\partial u/\partial z)^2 = \frac{1}{4}$ with a critical angle α_{crit} of the most unstable wave of about $\tan^{-1}(h/\lambda) = 7.6°$ (see Turner 1973, p. 99), where $\partial u/\partial z$ is the characteristic shear of a disturbance of wavelength λ and h is the vertical amplitude of the disturbance. By the Miles–Howard criterion, the dissipation rate of the embedded turbulence should be irrelevant to the instability process, especially when the wavelength of the saturated wave λ is very large compared to the size L of the embedded turbulent motions; that is, $\lambda \gg L_R > L > L_{KF}$.

The spectral form for saturated internal waves cannot be determined explicitly by dimensional analysis because the Gargett *et al.* (1981) assumption requires too many dimensional parameters. All that can be concluded is that $(k^2\phi_u)_{sat} = N^2L_Rf(kL_R)$ if it is assumed that $(k^2\phi_u)_{sat}$ is a function of ϵ, N and k. However, if the function $f(kL_R) = c(kL_R)^{-1}$, where c is a constant, as indicated by the Gargett *et al.* (1981) data, then the spectrum must have the form $(k^2\phi_u)_{sat} = cN^2k^{-1}$, which contradicts the assumption of a dependence on ϵ. Either the assumption is incorrect or the composite spectrum is incorrect or irrelevant.

The Miles–Howard instability criterion may be derived by considering a vertical perturbation of scale h over a horizontal distance λ of a horizontal flow with shear $\partial u/\partial z$ in a stratified fluid with density gradient $\partial\rho/\partial z$. An inertial force $F_I \sim \rho w^2\lambda^2$ arises which will tend to amplify the perturbation, where the vertical velocity $w \sim (\partial u/\partial z)h$. A buoyancy force $F_B \sim \Delta\rho\Delta Vg$ will tend to damp out the perturba-

tion, where $\Delta\rho \sim h(\partial\rho/\partial z)$ and $\Delta V \sim h\lambda^2$. Therefore $F_I \sim \rho(\partial u/\partial z)^2 h^2\lambda^2$ and $F_B \sim h(\partial\rho/\partial z)h\lambda^2 g$. For a saturated internal wave $F_I \approx F_B$, which gives $\rho(\partial u/\partial z)^2 \sim g(\partial\rho/\partial z)$, with a universal proportionality constant $(Ri)_{crit}^{-1}$. From this analysis we would expect the Richardson number $Ri = g(\partial\rho/\partial z)/\rho(\partial u/\partial z)^2$ of all saturated internal waves, with wavelength $\lambda > L_{KF}$, to have the same value $(Ri)_{crit}$. The characteristic value of shear squared $[\partial u/\partial z]^2(k)$ for motions in the spectral vicinity of wavenumber k is the shear spectrum $k^2\phi_u$ times the bandwidth $\Delta k = k$ (that is, the (shear)^2 over a bandwidth of one half octave). Therefore, for the saturated spectrum of (5) we find $[\partial u/\partial z]^2(k) = 6.7N^2$, or $[Ri(k)]_{sat} = 0.15$ which is close to the critical value of 0.25 for the most unstable waves in the Miles–Howard analysis. By the same procedure, we can estimate a characteristic Richardson number from the proportionally constant $0.45 = Ri^{-1}(k)$ for the k^{-1} subrange of the Gargett *et al.* (1981) composite spectrum, to give $Ri(k) = 2.2$, an order of magnitude larger than the critical value or 0.25. This is another indication that the composite spectrum is from fluid with subsaturated internal wave motions far below the transition to turbulence.

The saturated three-dimensional internal-wave locus of (5) is given by $(k^2\phi)_{KF} = 6.7(k)_{KF}^{-1}$, $(k)_{KF} < 1.05$, in the Gibson (1980) buoyancy coordinates, and is plotted on figure 3. Values of γ/N corresponding to various wave-turbulence transition wavenumbers k^* are shown along the equation (5) locus.

A line of constant $(k^2\phi)_{KF} = 10$ is shown in figure 3, with viscous cutoff at $(k)_{KF} \approx 1$. As discussed by Gibson (1980) and in §2, this constant level represents the spectrum for saturated (two–three)-dimensional internal wave motions, where it is assumed that the shear is not uniformly distributed but is concentrated in horizontal sheets of thickness $\approx L_{KF} = (\nu/N)^{\frac{1}{2}}$, separated vertically by the layer thickness $L_L \approx L_{KF}$, and the Richardson number of the motion on the sheets is near the critical value of $\frac{1}{4}$. If $L_L \gg L_{KF}$, a vertical cut through such a distribution of shear will show spikes of thickness L_{KF} at the sheets, separated by the layer thickness L_L. The normalized shear spectrum will be

$$(\phi_{[\partial u/\partial z]})_{KF} \approx 10\left[\frac{L_L}{L_{KF}}\right], \tag{13}$$

for wavelengths larger than about $2L_L$ with a k^{-1} subrange for smaller wavelengths out to the viscous cutoff at L_{KF}. A high wavenumber rolloff of the k^{-1} subrange should begin at $k \approx (N/\nu)^{\frac{1}{2}}$, as discussed by Gibson (1980, 1981*a*). The white portion of the shear spectrum corresponding to (13) is

$$\phi_{[\partial u/\partial z]} \approx 10\nu^{\frac{1}{2}}N^{\frac{3}{2}}\left[\frac{L_L}{L_{KF}}\right],$$

which shows that viscosity may play a role in determining the levels of high-wavenumber internal wave motions, a possibility which apparently has not been put forward previously (oceans of stratified molasses being rare). The lengthscale L_{KF} is the natural viscous cutoff scale of internal waves, just as L_K is the natural viscous cutoff scale of turbulence.

We see from figure 3 that the composite shear spectrum has features which resemble the saturated two-dimensional and three-dimensional wave spectra and the universal turbulence spectra, but the levels do not match any of these spectra in any subrange. From the comparison we conclude that the microstructure range is fossil turbulence, except for a narrow range near the peak of the bump and that the k^{-1} range represents subsaturated (two–three)-dimensional internal waves on sheets separated by layers two or three metres thick.

4. The schematic temperature-gradient spectrum of Gregg (1977) compared with the spectral theory of Gibson (1980)

If a saturated-three-dimensional-internal-wave spectrum is imposed on a thermally stratified fluid with constant N, the resulting temperature fluctuations may be expected to reflect the isotropy of the saturated waves. The amplitude of the temperature-gradient spectrum should depend only on the wavenumber k and the vertical temperature gradient $\partial\bar{T}/\partial z$. By dimensional analysis $k^2\phi_T = d(\partial\bar{T}/\partial z)^2 k^{-1}$, $L_L^{-1} < k < L_{KB}^{-1}$, where d is a universal constant. Subsaturated internal waves acting on a uniform temperature gradient should produce an anisotropic temperature field, with $k^2\phi_T = d'(\partial\bar{T}/\partial z)^2 k^{-1}$, but with d' less than d. In a collection of measured d' values, if any of the data represents saturated internal waves then $d = \max d'$.

Gregg (1977) presents a large number of measured temperature-gradient spectra which are reproduced in figure 4, from which the constant d can be estimated by taking the maximum d' value. As shown in figure 4, the value $\bar{d} = 0.18$ used in Gregg's schematic spectrum of figure 1 represents an average value of d' in the depth range 200–400 m, rather than a maximum value. Values of d' indicated by most of the spectra are much larger than 0.18, especially for the spectra with wide microstructure subranges. From the data of figure 4, Gibson (1980) estimates $d = 0.9$. The wide scatter of d' values over a range of (0.1–1.0), from figure 3, indicates that the Gregg schematic $k^{-1.1}$ spectral subrange probably represents subsaturated rather than saturated internal waves. This interpretation is supported by the test for isotropy given in figure 17, p. 452 of Gregg (1977) which shows that typical microstructure spectra from the data set are almost completely vertically stratified at the transition wavenumber k^*. Therefore the microstructure near k^* is certainly not turbulent and the internal-wave-induced temperature spectrum is not saturated.

An independent method of estimating d is described in Gibson (1982*b*), leading to (12) and (15) below. The method is similar to the derivation of (5) in §2. We assume that the saturated temperature-gradient internal-wave spectrum coincides with the beginning of the turbulent scalar inertial subrange at fossilization; that is

$$k^2\phi_{T\text{satd int. waves}} = [k^2\phi_T]^*_{\text{turbulence}} = \beta_K \chi_0 \epsilon_0^{-\frac{1}{3}} k^{\frac{1}{3}}, \quad k = k_0^*, \tag{14}$$

where $\beta_K = 0.5$, $k_0^* = (2\pi/1.2)N^{\frac{3}{2}}\epsilon_0^{-\frac{1}{2}}$ and 0-subscripts indicate turbulence at the point of fossilization.

For entraining turbulence at the point of fossilization $\chi_0 \sim (\Delta T)^2 N \sim (\epsilon_0/N^2)(\partial\bar{T}/\partial z)^2$ with a proportionality constant of about 0.16. The constant 0.16 is found from the boundary condition that at transition, where $(\epsilon_0)_{tr} \approx 25\,\nu N^2$, the Cox number should be about $2(\nu/D)$ (see Gibson 1982*b*, 1986 for further discussion). Substituting $\chi_0 = 0.16(\epsilon_0/N^2)(\partial\bar{T}/\partial z)^2$ in (14) gives $d = (0.16\beta_K)(2\pi/1.2)^{\frac{1}{3}} = 0.72$. Therefore, we expect the universal temperature-gradient spectrum for three-dimensional saturated internal waves to have the form

$$k^2\phi_T(k) = (0.7 \pm 0.3)\left(\frac{\partial\bar{T}}{\partial z}\right)^2 k^{-1}; \quad L_L^{-1} < k < k_0^*, \tag{15}$$

where k_0^* represents the transition wavenumber of turbulence at fossilization, past or present, with maximum dissipation rate ϵ_0. Most of the uncertainty range is due to uncertainty in the buoyancy–inertial transition wavenumber. The saturated three-dimensional subrange of (15) is shown in figure 4 as a dash–dot–dash line. It agrees rather well with the spectra with the most extensive microstructure subranges, which should represent the regions with the most recent or active turbulence.

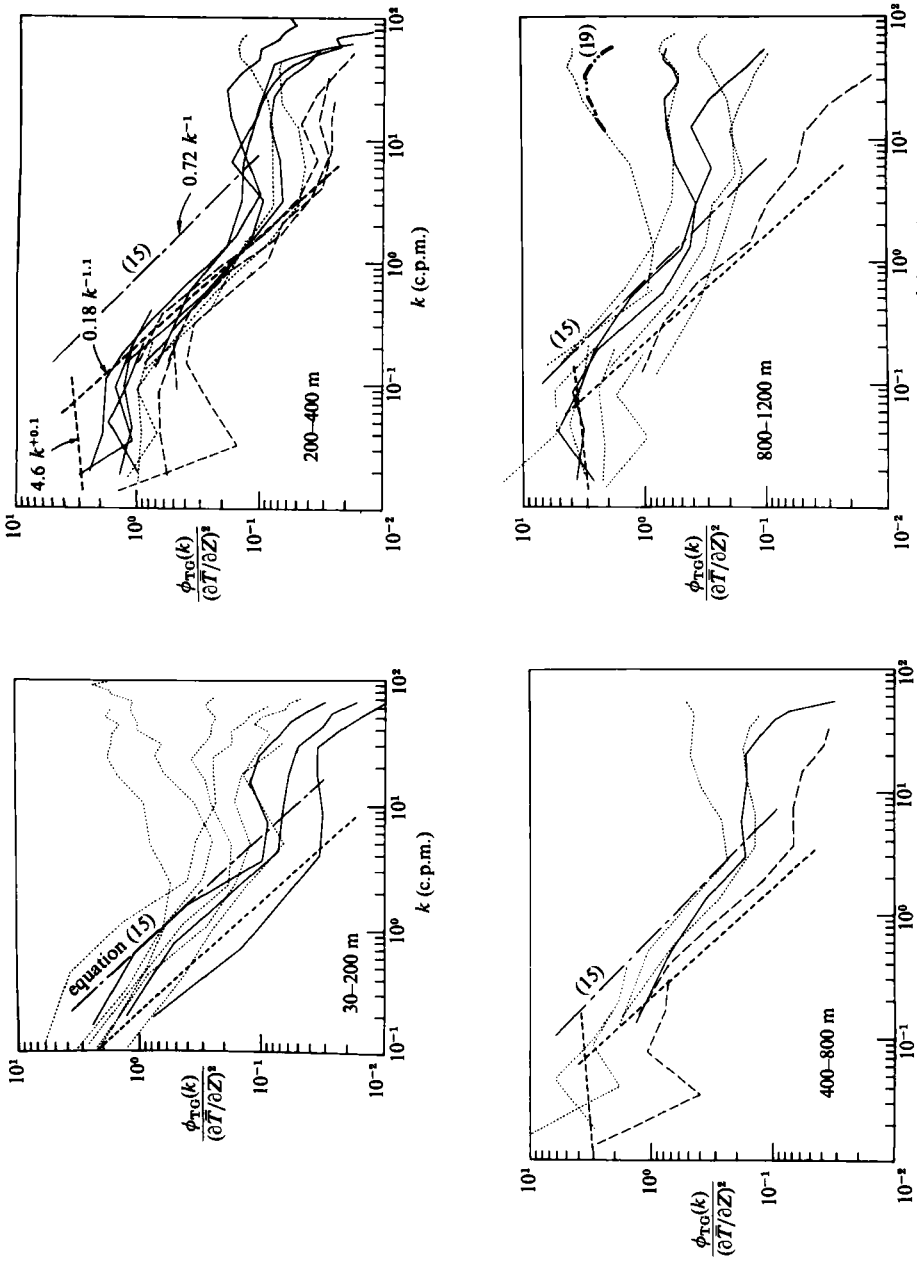

FIGURE 4. Temperature-gradient spectra normalized with $(\partial\bar{T}/\partial z)^2$ for various depth ranges at 28 °N 155 °W, from Gregg (1977). The saturated three-dimensional internal-wave subrange of equation (15) (dash–dot–dash line) is in best agreement with spectra with the most extensive microstructure subranges, indicating recent turbulence. The Gregg (1977) schematic spectrum $0.18k^{-1.1}$ (dashed line) apparently represents subsaturated (two–three)-dimensional internal waves. Most of the microstructure spectra represent fossil temperature turbulence in an advanced state of decay when compared to the Gibson (1980) spectra model. The spectra have been overcorrected for thermistor frequency response. An improved response correction, from Baker (1985), is shown for drop Tasaday 11 (19) which encountered the most active patch detected. – –, Aires 9; ——, Tasaday 1; ·····, Tasaday 11.

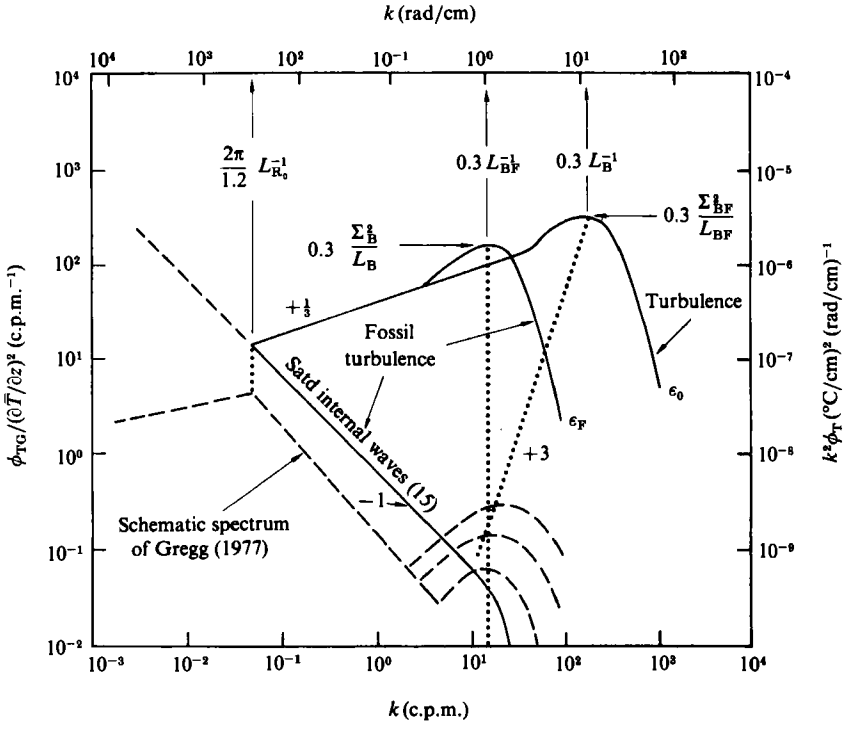

FIGURE 5. Schematic temperature-gradient spectra of Gregg (1977) compared with universal spectral forms for stratified turbulent mixing of Gibson (1980). Radian wavenumber axes are shown at the right and top. A turbulent temperature-gradient spectrum is shown corresponding to the dissipation rate $\epsilon_0 = 0.067$ cm^2/s^3, as well as the fossil-temperature-turbulence spectrum which should result when the turbulence is damped according to the Gibson (1980) model, with dissipation $\epsilon_F = (5N)^2\nu = 3.8 \times 10^{-6}$ cm^2/s^3. Peak values are shown in terms of the Batchelor (1959) turbulent mixing scales and the Gibson (1980) fossil-temperature-turbulence scales.

Figure 5 shows a comparison between the schematic temperature-gradient spectrum of Gregg (1977) and the saturated-internal-wave spectrum of (15), with diffusive cutoff at the diffusive–buoyancy scale $L_{BF} = (D/N)^{\frac{1}{2}}$, as proposed by Gibson (1980). Also shown in figure 5 are the universal turbulent-temperature-gradient spectrum corresponding to the dissipation rate ϵ_0 and the fossil-temperature-gradient spectrum corresponding to $\epsilon_F = 25\nu N^2$, where ϵ_0 is inferred from the transition wavenumber $k_0 = k_0^*$ rad/cm. The spectra are shown without normalization by the mean temperature gradient as a function of radian wavenumber $k = 2\pi/\lambda$ with axes shown at the top and right, using the conditions from the depth range 800–1200 m, where $\partial\bar{T}/\partial z = 2.5 \times 10^{-3}$ °C/m, $N = 3.6 \times 10^{-3}$ rad/s and $k_0^* = 0.07$ c.p.m.

The transition k_0^* is found by equating the Gregg (1977) schematic subranges $4.6k^{0.1} = 0.18k^{-1.1}$, giving $k_0^* = \exp[\ln(0.18/4.6)/1.2] = 0.067$ c.p.m. Therefore the dissipation rate at fossilization corresponding to the indicated mixed-layer thickness is $\epsilon_0 = (\frac{100}{1.2} \times 0.07)^2\ (3.6 \times 10^{-3})^3 = 6.6 \times 10^{-2}$ cm^2/s^3. The rate of strain $\gamma_0 = (\epsilon_0/\nu)^{\frac{1}{2}} = 2.35$ s^{-1}, which gives $\gamma_0/N = 651$, and ϵ_F is 4.4×10^{-6} cm^2/s^3.

The universal turbulent scalar gradient spectrum consists of an inertial subrange, with

$$k^2\phi_T = \beta_K \chi \epsilon^{-\frac{1}{3}} k^{\frac{1}{3}}, \tag{16}$$

Field	Quantity	Turbulence	Fossil turbulence
Velocity	Length	$L_K = (\nu/\gamma)^{\frac{1}{2}}$	$L_{KF} = (\nu/N)^{\frac{1}{2}}$
	Time	$T_K = \gamma^{-1}$	$T_{KF} = N^{-1}$
Scalar	Length	$L_B = (D/\gamma)^{\frac{1}{2}}$	$L_{BF} = (D/N)^{\frac{1}{2}}$
	Time	$T_B = \gamma^{-1}$	$T_{BF} = N^{-1}$
	Scalar	$\Sigma_B = (\chi/\gamma)^{\frac{1}{2}}$	$\Sigma_{BF} = (\chi/N)^{\frac{1}{2}}$

TABLE 2. Universal similarity scales for turbulence, turbulent mixing, and fossil turbulence

and the viscous–convective and diffusive cutoff subrange of Batchelor (1959),

$$k^2\phi_T = \beta_B\chi\gamma^{-1}k\left[\exp(-\tfrac{1}{2}\alpha^2) - \alpha\int_\alpha^\infty \exp(-\tfrac{1}{2}y^2)\,dy\right], \tag{17}$$

where $\beta_K = 0.5$ and $\alpha = k(2\beta_B D/\gamma)^{\frac{1}{2}}$ (see Gibson & Schwarz 1963). The universal constant β_B is in the range $\sqrt{3} < \beta_B < 2\sqrt{3}$, as shown by Gibson (1968, 1982*b*). The spectrum has a peak value at wavenumber $k_p = 0.60/(2\beta_B)^{\frac{1}{2}}(D/\gamma)^{\frac{1}{2}}$, with value $(k^2\phi_T)_p = 0.254\ (\frac{1}{2}\beta_B)^{\frac{1}{2}}\chi(\gamma D)^{-\frac{1}{2}}$. Substituting the range of possible β_B values gives $k_p = (0.32\text{–}0.23)(\gamma/D)^{\frac{1}{2}}$ and $(k^2\phi_T)_p = (0.24\text{–}0.33)\,\chi(\gamma D)^{-\frac{1}{2}}$. In figure 5 the universal peak values are shown as $k_p = 0.3(\gamma/D)^{\frac{1}{2}}$ and $(k^2\phi_T)_p = 0.3\chi(\gamma D)^{-\frac{1}{2}}$, for simplicity. The locus of peak values at fossilization $[(k^2\phi_T)_p, k_p]_0$ forms a line of slope +3 on a log–log plot for patches with different γ_0/N values, as shown by a dashed line in figure 5. In terms of the Batchelor temperature scale $\Sigma_B = (\chi/\gamma)^{\frac{1}{2}}$ and Batchelor lengthscale $L_B = (D/\gamma)^{\frac{1}{2}}$ the peak is $(0.3\Sigma_B^2 L_B^{-1},\ 0.3L_B^{-1})$, which is also indicated.

According to the fossil-turbulence model of Gibson (1980) the temperature-gradient spectrum at large scales should not be very much changed during the process of buoyant damping of the turbulence, which should take a time period about N^{-1}, but the peak value for a given patch should follow a locus of slope $+\frac{1}{3}$ to a final value of $(0.3\Sigma_{BF}^2 L_{BF}^{-1},\ 0.3L_{BF}^{-1})$ as the rate of strain of the turbulence decreases from the value at fossilization γ_0 to the buoyant–viscous transitional value of $\gamma_F = 5N$. The evolution of the fossil-temperature-turbulence spectrum for times larger than N^{-1} should be a gradual vertical decay of the original fossil-turbulence spectrum in figure 5, with the peak maintained at wavenumber $k = 0.3(\gamma/D)^{\frac{1}{2}}$ by the rate of strain $\gamma < 5N$ of the laminar internal wave and restratification motions of the fossil turbulence. The peak values of the Gregg (1977) microstructure spectra are close to the $0.3L_{BF}^{-1}$ wavenumber, which shows they are from fluid in a fossil-turbulence state. Baker (1985) has corrected the peak values of these spectra for thermistor frequency response, as shown for Tasaday 11 (19) in figure 3 and discussed in §5. A summary of various universal length-time- and scalarscales for turbulence, turbulent mixing and fossil-turbulence velocity and scalar fields is given in table 2 (for details see Gibson 1968, 1980 and the discussion in §2).

5. Layer thicknesses and previous turbulence activity

In this section we shall explore the implications of the assumption that the layer thicknesses indicated by the transition wavenumbers k_0^* in the composite and schematic spectra of figure 1 represent partially mixed layers in the ocean interior produced by previous turbulence events.

Depth range (m)	N (rad/s)	$\partial\overline{T}/\partial z$ (°C/m)	k_0^*, (c.p.m.)	ϵ_0 cm²/s³ (18)	χ_0 °C²/s (19)	C_0 (20)
30–200	7.7×10^{-3}	4.0×10^{-2}	0.10	0.32	1.3×10^{-4}	3.0×10^{5}
200–400	5.3×10^{-3}	3.0×10^{-2}	0.10	0.10	4.9×10^{-5}	2.0×10^{5}
400–800	4.0×10^{-3}	1.0×10^{-2}	0.10	0.044	4.2×10^{-6}	1.5×10^{5}
800–1200	3.6×10^{-3}	2.5×10^{-3}	0.07	0.066	4.9×10^{-7}	1.2×10^{6}

TABLE 3. Turbulence parameters ϵ_0, χ_0, and C_0 assuming layers of Gregg (1977) data are produced by previous turbulent mixing.

From figure 3 we see that the transition wavenumber k_0^* between the $k^2\phi_T \sim k^0$ and $\sim k^{-1}$ subranges for the Gregg (1977) data is actually somewhat depth dependent. The transition between $4.6k^{0.1}$ and $0.18k^{-1.1}$ subranges of the schematic temperature-gradient spectrum occurs at k_0^* of 6.7×10^{-2} c.p.m. However, only the spectra from the deepest layers, at 800–1200 m, exhibit this transition. All the other depth ranges show a transition at about $k_0^* = 0.1$ c.p.m.

As mentioned previously, the physical significance of the transition wavenumber k_0^* has not been conclusively demonstrated, but a strong possibility is that k_0^* reflects the thickness of layers, and a reasonable speculation is that the layer thickness is determined by previous turbulence activity. The intensity of the turbulence necessary to produce layers of thickness 5–10 m is very large compared to that measured by Gregg (1977), as shown by Gibson (1982*a*). If we identify k_0^* with $1/\lambda_0$, where $\lambda_0 = 1.2L_{R_0}$, $L_{R_0} = (\epsilon_0/N^3)^{\frac{1}{2}}$ and ϵ_0 is the dissipation rate of the turbulence at fossilization which produced the mixed layer, then

$$\epsilon_0 = \left(\frac{100}{1.2k_0^*}\right)^2 N^3, \tag{18}$$

where k_0^* is in c.p.m., N is in rad/s and ϵ_0 is in cm²/s³. The temperature-variance dissipation rate at fossilization may also be estimated from an expression

$$\chi_0 = \frac{2}{13}\left(\frac{\epsilon_0}{N^2}\right)\left(\frac{\partial\overline{T}}{\partial z}\right)^2, \tag{19}$$

from Gibson (1980). The Cox number at fossilization

$$C_0 = \frac{\chi_0}{2D(\partial\overline{T}/\partial z)^2}, \tag{20}$$

may also be calculated.

Table 3 gives values of ϵ_0, χ_0 and C_0 for the various depth ranges studied by Gregg (1977) calculated using the preceding expressions (18), (19) and (20) and the assumption that k_0^* represents a fossil-turbulence mixing-layer thickness. N values were inferred from the T–S diagram and temperature profile given by Gregg (1977) and are in the range $(3.6\text{–}7.7)\times10^{-3}$ rad/s in the (30–1200) m range of depths sampled. Resulting ϵ_0 values are in the range $(4\text{–}30)\times10^{-2}$ cm²/s³, with slightly larger values in the 30–40 m depth range compared to values at 400–1200 m. Layer χ_0 values show a more systematic depth dependence, decreasing from 1.3×10^{-4} °C²/s for the (30–200) m range to only 4.9×10^{-7} °C²/s for (800–1200) m. Cox numbers C_0 were relatively constant near 2×10^5, except for a larger value of 1.2×10^6 for the deepest range.

Depth interval (m)	C_0	$\bar{C} \pm \sigma\,(n)$	A_S %
30–200	3.0×10^5	43 ± 45 (11)	1.8
200–400	2.0×10^5	9.1 ± 7.8 (10)	0.5
400–800	1.5×10^5	31 ± 43 (10)	1.2
800–1200	12×10^5	56 ± 77 (8)	0.5

TABLE 4. Cox numbers and adequacy of sample A_S, Gregg (1977) data.

Table 4 gives a comparison between the C_0 values of table 3 and the average measured values $\bar{C} \pm \sigma(n)$, where $\bar{C}$ is the average measured Cox number in the depth range, σ is the standard deviation of the measured values and n is the number of 100–200 m length dropsonde samples averaged. As shown in table 4, the $\bar{C}$ values are much smaller than C_0, by factors of $(6–30) \times 10^3$. Also shown in table 4 is a measure of the adequacy of the sample A_S,

$$A_S \equiv \left(\frac{\bar{C}}{C_0}\right)\left(\frac{L_{\text{sample}}}{L_{\text{layer}}}\right) 100, \tag{22}$$

where L_{sample} is the record length of the sample from which $\bar{C}$ was calculated and L_{layer} is the layer thickness $L_{\text{layer}} \approx (2k_0^*)^{-1}$.

The adequacy of sampling parameter A_S is based on the assumption that the sample is inadequate unless it contains at least one sample of the fully turbulent patches which produce the internal mixed layers reflected by k_0^*. Such a turbulent patch must be at least $L_L = (2k_0^*)^{-1}$ in length with a Cox number of at least C_0, and the average $\bar{C}$ for the total sample must be at least as large as $C_0(L_L/L_S)$. Therefore if the measured sample average $\bar{C}$ is less than $C_0(L_L/L_S)$ the sample record cannot contain an actively turbulent patch with $C > C_0$ so that A_S must be less than 100 %. A_S values in table 4 are quite small, between $\frac{1}{2}$ and 2 %. Therefore, if the C_0 values actually reflect previous turbulence intensities, then the sample record lengths of the Gregg (1977) data are inadequate by factors of 100 or more.

An important topic for future studies of ocean turbulence and mixing is to determine the statistical laws describing the distribution of the turbulence parameters ϵ, χ and C in space and time for various ocean layers. Preliminary evidence (Gibson 1981*a*; Williams 1974; Elliott & Oakey 1979; Washburn & Gibson 1984) suggests that $X = \epsilon$, χ, or C may be lognormal. However, the variance of ln X seems to increase with the length of record sampled, and differs from region to region. The sampling problem is complicated by a tendency for the most active patches to cluster in 'clouds' in space and 'storms' in time, so that individual samples must be widely separated in space and time in order that they be statistically independent. Knowledge of the statistical laws and the correlation lengths and times are necessary before one can be confident that the microstructure measurement sample size is adequate for the mean values to converge.

A recent study by Baker (1985) and Baker & Gibson (1986) shows that microstructure data sets from the seasonal thermocline, main thermocline and equatorial undercurrent layers have dissipation parameters X that are extremely intermittent with probability distribution functions indistinguishable from lognormal. The intermittency factor $\sigma^2_{\ln X}$ ranges from 3 to 7 in these layers (corresponding to kurtosis values of 20–1100 for velocity and temperature gradients if the X are lognormal), so that egregious underestimates of mean values are *probable* if the intermittent lognormality of the dissipation rates is ignored. The 95 % confidence interval for the maximum likelihood

estimator of the mean $\bar{C}_{\mathrm{mle}}$ of the 150 m Gregg (1977) $\bar{C}$ samples in the depth interval 600–1200 m (below the salinity minimum so double diffusive effects are small) is 62–2600, using the observed lognormality of the data and the indicated value $\sigma^2_{\ln C} = 5.4$. The $\bar{C}_{\mathrm{mle}}$ value for the 10 samples is 418, which shows there is no statistically significant discrepancy between the Gregg (1977) measurements and eddy diffusivity estimates of $\bar{C} \approx 700$ based on bulk property models such as Munk (1966). A large discrepancy between this value and $\bar{C}$ estimates from the microstructure data, by factors of 10–100, is proposed by Gregg (1977) Gregg & Briscoe (1979) and others, and is widely accepted in the oceanographic community.

Baker (1985) recorrects the Gregg (1977) spectra and $\bar{C}$ values for thermistor frequency response. The original spectra are substantially overcorrected, so that some of the more active spectra shown in figure 4 appear to be cut off by thermistor response rather than thermal diffusivity. The recorrected $\bar{C}$ values are reduced by factors as large as two and the recorrected spectra all show well-resolved diffusive rolloff peaks $k_{\mathrm{p}} = 0.3(\gamma/D)^{\frac{1}{2}}$ (see figure 3), so that the strain rates γ can be estimated. The most active (in terms of χ) microstructure patch observed by Gregg (1977) is from drop Tasaday 11 (20), with original and recorrected spectra shown in figure 4. The recorrected diffusive peak $k_{\mathrm{p}} = 30$ c.p.m. gives $\epsilon = 3.7 \times 10^{-5}$ cm^2/s^3, so $\gamma/N \approx 18$. This is somewhat greater than 5, so the patch appears to be actively turbulent for temperature fluctuations with wavelengths from 7–40 cm, and fossil turbulence for wavelengths of 40–2000 cm. The A^0_{T} value is 0.02 from (2*c*) using the ϵ_0 value from table 3. Caldwell (1983), Dillon (1984) and Gregg (1984) have questioned the Gibson (1982*a*) interpretation of the most active Gregg (1977) microstructure patch, from drop Tasaday 11 (19), as fossil temperature turbulence based on their assumption that the thermistor did not resolve the diffusive cutoff peak k_{p} of the temperature-gradient spectrum. This assumption appears to be unjustified based on the Baker (1985) recorrected spectrum.

6. Summary and conclusions

Comparisons of the composite shear spectrum of Gargett *et al.* (1981) and the schematic temperature-gradient spectrum of Gregg (1977) with universal spectral forms for active turbulence and temperature mixing predicted by the Gibson (1980–86) fossil-turbulence model show that the ocean layers sampled were essentially non-turbulent at the time of measurement. The forms of the measured spectra suggest that strong previous turbulence and turbulent mixing activity have occurred leaving remnant subsaturated internal waves and temperature microstructure, termed fossil vorticity turbulence and fossil temperature turbulence, respectively, by Gibson (1980). In the most active χ patch measured, Tasaday 11 (19), temperature fluctuations are fossil on wavelengths between 40 and 2000 cm, with turbulent motions confined to a range of wavelengths of only about 7–40 cm. Because the data sets do not include actively turbulent patches which caused the fossil turbulence remnants, the turbulence and turbulent mixing processes have been (vastly) undersampled.

The Gargett *et al.* (1981) composite shear spectrum has a k^{-1} subrange of $0.45N^2\,k^{-1}$, far below the Gibson (1980–1986) saturated-three-dimensional-internal-wave subrange $(6.6 \pm 1.8)N^2\,k^{-1}$, as shown in figure 3, indicating subsaturated-internal-wave motions possibly caused by buoyant damping of strong previous turbulence. Because the velocity microstructure subrange indicates rates of strain γ only slightly larger than the minimum required for turbulence of $5N$, the Gargett *et al.* (1981) microstructure subrange is essentially non-turbulent internal wave motions at the time of sampling

and may be classified as fossil vorticity turbulence, using the Gibson (1980) nomenclature. The Gargett *et al.* (1981) buoyancy scaling hypothesis for the k^{-1} subrange is shown to be physically implausible and the assumption of an ϵ dependence is inconsistent with the observed form of the subrange on dimensional grounds.

The schematic temperature-gradient spectrum of Gregg (1977) also exhibits a k^{-1} subrange. As shown in figure 5, the level $0.18(\partial\overline{T}/\partial z)^2 k^{-1.1}$ is well below the Gibson (1980) universal saturated three-dimensional internal-wave level of (0.7 ± 0.3) $(\partial\overline{T}/\partial z)^2 k^{-1}$, suggesting subsaturated internal waves. The microstructure peaks occur at wavenumbers very close to the value of $0.3L_{\mathrm{BF}}^{-1}$ expected for fossil temperature turbulence, where $L_{\mathrm{BF}} = (D/N)^{\frac{1}{2}}$ is the microscale of fossil turbulence for a scalar property of diffusivity D proposed by Gibson (1980). Because Gregg (1977) determined that the larger wavelengths of the schematic temperature-gradient microstructure spectrum is usually strongly anisotropic and stratified in the vertical, the fluid cannot be actively turbulent at these scales. Rather, the spectra of figure 3 and the schematic representation of figures 1 and 5 probably represent fossil temperature turbulence and fossil vorticity turbulence in an advanced state of decay.

Consequences were explored of the reasonable speculation that the transition wavenumber $k^* \approx 0.1$ c.p.m., which appears as a striking feature in both the composite shear and schematic temperature gradient spectra, is actually a fossil remnant of previous turbulence events which have produced partially mixed layers in the ocean interior. Temperature profiles in the deep ocean have a definite step-like structure, and the thickness of the steps is apparently reflected by the transition between k^0 and k^{-1} subranges at the 'turbulence-at-fossilization' wavenumber k_0^* in both the temperature-gradient and velocity-shear spectra. If the turbulent mixing events were recent, the wavenumber k_0^* should be approximately equal to $2\pi/\lambda_0$, where $\lambda_0 = 1.2L_{\mathrm{R}_0} = 1.2(\epsilon_0/N^3)^{\frac{1}{2}}$, and ϵ_0 is the dissipation rate of the turbulence necessary to mix a layer of thickness about $\frac{1}{2}\lambda_0$ on a fluid of Väisälä frequency N. Turbulence parameters ϵ_0, χ_0, and C_0 corresponding to the mixed-layer thickness inferred from k_0^* in various layers of the Gregg (1977) study are given in table 3. The ϵ_0 values range from 0.32 cm^2/s^3 above 200 m depth to about 0.05 cm^2/s^3 at a kilometre. Shallow χ_0 values are over 10^{-4} °C^2/s and decrease to 5×10^{-7} °C^2/s at a kilometre depth. These values are much larger than the dissipation rates ϵ of $(7\text{–}39)\times10^{-6}$ cm^2/s^3 measured by Gargett *et al.* (1981) or the range of χ values (10^{-7} to 10^{-12}) °C^2/s, measured by Gregg (1977). Similarly, the Cox numbers C_0 are $(12\text{–}2)\times10^5$, which is about 10^4 larger than the 150 m averaged measured values of $\overline{C}$ presented by Gregg (1977). Such large Cox numbers C_0 suggest that the turbulence process has been severely undersampled. An 'adequacy-of-sample' parameter A_{S} is defined in §4, and has values of less than 2 % for the layers sampled by Gregg (1977). Because restratification and vertical diffusion processes will tend to reduce the apparent fossil mixed-layer thickness, the ϵ_0, χ_0, and C_0 parameters in table 3 represent lower bounds of larger actual values, and the A_{S} values of table 4 may also be too large for the same reasons.

Because no actively turbulent patches with vertical turbulence scales as large as the average layer thickness of about 5 m have been observed, the speculation that the layer thickness is a fossil remnant of previous turbulence is unconfirmed. However, the Gregg (1980) observation of Thorpe vertical overturning scales from 3 to 7.5 m within layers of about the same vertical thickness seems to support this assumption rather strongly. Oakey & Elliott (1980) report Cox numbers as large as those inferred in table 3, but have not computed Thorpe displacement scales or estimated the average layer thickness for their data. Both the Gregg (1977) and Oakey

& Elliott (1980) data suggest that microstructure activity is rather poorly correlated with the location of double diffusive instability of the water column.

Perhaps the most important conclusion to be drawn from the preceding discussion is that the study of the turbulence and turbulent mixing processes of the ocean is in a very early stage. The very wide bandwidth composite and schematic spectra assembled by Gargett *et al.* (1981) and Gregg (1977) provide a valuable first look. The spectra reveal the complexity of the phenomena and the need for much larger data sets with high-frequency response and high-resolution sensors. Better fluid mechanical models of stratified turbulence are needed, with quantitative statistical descriptions of the flow regimes and reduced uncertainty ranges for the universal constants and spectral forms, verified wherever possible by controlled laboratory experiments and field studies. It is clear that the turbulence and turbulent mixing process in the deep ocean is very patchy in space and intermittent in time, but only the most rudimentary quantitative descriptions of the degree of patchiness and intermittency are available. Consequently, at this time it is fair to say that the average vertical diffusivities, viscous dissipation rates and temperature dissipation rates characteristic of the deep ocean and many important layers are still unknown to within factors of perhaps 1–3 orders of magnitude.

Support was provided by a grant from UCSD Committee on Research and by the Office of Naval Research. The author is grateful to Ann Gargett for making the composite shear spectrum manuscript available at an early stage, and for several useful discussions with colleagues and students, especially Libe Washburn, Mark Baker, Ann Gargett and Mike Gregg. This paper is dedicated to the memory of John C. Schedvin, whose contributions were invaluable in the early development of the stratified turbulence and mixing ideas presented herein, and the towed body measurements from which these ideas derived. The editor has informed the author that a particularly extensive and valuable first review of the present paper was provided by John Schedvin.

REFERENCES

Baker, M. A. 1985 Sampling turbulence in the stratified ocean: statistical consequences of strong intermittency. Ph.D. dissertation, University of California at San Diego.

Baker, M. A. & Gibson, C. H. 1986 Sampling turbulence in the stratified ocean: statistical consequences of strong intermittency. Submitted for publication.

Batchelor, G. K. 1959 Small-scale variation of convected quantities like temperature in a turbulent fluid. *J. Fluid Mech.* **5**, 113–133.

Caldwell, D. R. 1983 Oceanic turbulence: big bangs or continuous creation? *J. Geophys. Res.* **88**, C12, 7543–7550.

Caldwell, D. R., Dillon, T. M., Brubaker, J. M., Newberger, P. A. & Paulson, C. A. 1980 The scaling of vertical temperature spectra. *J. Geophys. Res.* **85**, 1917–1924.

Champagne, F. H. 1978 The fine-scale structure of the turbulent velocity field. *J. Fluid Mech.* **86**, 67–108.

Crawford, W. R. 1982 Pacific equatorial turbulence. *J. Phys. Oceanogr.* **12**, 1137–1149.

Dillon, T. R. 1982 Vertical overturns: a comparison of Thorpe and Ozmidov length scales. *J. Geophys. Res.* **87**, C12, 9601–9613.

Dillon, T. R. 1984 The energetics of overturning structures: implications for the theory of fossil turbulence. *J. Phys. Oceanogr.* **14**, 541.

Dillon, T. R. & Caldwell, D. R. 1980 The Batchelor spectrum and dissipation in the upper ocean. *J. Geophys. Res.* **85**, C4, 1910–1916.

ELLIOTT, J. A. & OAKEY, N. S. 1979 Average microstructure levels and vertical diffusion for Phase III, GATE. *Oceanography and Surface Layer Meteorology in the B/C-Scale* (ed. G. Siedler & J. D. Woods), GATE vol. 1, pp. 273–294. Pergamon.

GARGETT, A. E. 1985 Evolution of scalar spectra with the decay of turbulence in a stratified fluid. *J. Fluid Mech.* **159**, 379–407.

GARGETT, A. E., HENDRICKS, P. J., SANFORD, T. B., OSBORN, T. R. & WILLIAMS, A. J. 1981 A composite spectrum of vertical shear in the upper ocean. *J. Phys. Oceanogr.* **11**, 1258–1271.

GIBSON, C. H. 1968 Fine structure of scalar fields mixed by turbulence: I. Zero-gradient points and minimal gradient surfaces; II. Spectral theory. *Phys. Fluids* **11**, 2305–2315, 2316–2327.

GIBSON, C. H. 1980 Fossil temperature, salinity, and vorticity turbulence in the ocean. In *Marine Turbulence* (ed. J. C. J. Nihoul), pp. 221–257. Elsevier.

GIBSON, C. H. 1981*a* Fossil turbulence and internal waves. In *American Institute of Physics Conference Proceedings No. 76: Nonlinear Properties of Internal Waves* (ed. B. West), pp. 159–179.

GIBSON, C. H. 1981*b* Buoyancy effects in turbulent mixing: sampling the stratified ocean. *AIAA J.* **19**, 1394–1400.

GIBSON, C. H. 1982*a* Alternative interpretations for microstructure patches in the thermocline. *J. Phys. Oceanogr.* **12**, 374–383.

GIBSON, C. H. 1982*b* On the scaling of vertical temperature gradient spectra. *J. Geophys. Res.* **87**, C10, 8031–8038.

GIBSON, C. H. 1982*c* Fossil turbulence in the Denmark Strait. *J. Geophys. Res.* **87**, C10, 8039–8046.

GIBSON, C. H. 1983 Turbulence in the equatorial undercurrent core. In *Hydrodynamics of the Equatorial Ocean* (ed. J. C. H. Nihoul), vol. 36, p. 131–154. Elsevier.

GIBSON, C. H. 1986 Ocean turbulence; big bangs and continuous creation. *J. Physico Chem. Hydrodyn.* (in press).

GIBSON, C. H. & SCHWARZ, W. H. 1963 The universal equilibrium spectra of turbulent velocity and scalar fields. *J. Fluid Mech.* **16**, 365–384.

GRANT, H. L., STEWART, R. W. & MOILLIET, A. 1962 Turbulence spectra from a tidal channel. *J. Fluid Mech.* **12**, 241–268.

GREGG, M. C. 1977 Variations in the intensity of small scale mixing in the main thermocline. *J. Phys. Oceanogr.* **1**, 436–454.

GREGG, M. C. 1980 Microstructure patches in the thermocline. *J. Phys. Oceanogr.* **10**, 915–943.

GREGG, M. C. 1984 Persistent turbulent mixing and near-inertial internal waves. *Internal Gravity Waves and Small-Scale Turbulence: Proceedings, January 17–20, 1984* (ed. P. Muller & R. Pujalet), pp. 1–24. Hawaii Institute of Geophysics, Honolulu.

GREGG, M. C. & BRISCOE, M. G. 1979. Internal waves, finestructure, microstructure, and mixing in the ocean. *Rev. Geophys. Space Phys.* **17**, 1524–1548.

GREGG, M. C. & SANFORD, T. B. 1980 Signatures of mixing from the Bermuda Slope, the Sargasso Sea and the Gulf Stream. *J. Phys. Oceanogr.* **10**, 105–127.

GREGG, M. C. & SANFORD, T. B. 1981 Reply. *J. Phys. Oceanogr.* **11**, 1438–1439.

HOWARD, L. N. 1961 Note on a paper of John W. Miles. *J. Fluid Mech.* **10**, 509.

ITSWEIRE, E. C., HELLAND, K. N. & VAN ATTA, C. W. 1986 The evolution of a grid-generated turbulence in a stably stratified fluid. *J. Fluid Mech.* **162**, 299–338.

KOLMOGOROFF, A. N. 1941 The local structure of turbulence in incompressible viscous fluid for very large Reynolds number. *Dokl. Akad. Nauk SSSR* **30**, 301.

LANFORD, O. E. 1982 The strange attractor theory of turbulence. *Ann. Rev. Fluid Mech.* **14**, 347–365.

MILES, J. W. 1961 On the stability of heterogeneous shear flows. *J. Fluid Mech.* **10**, 496.

MUNK, W. H. 1966 Abyssal recipes. *Deep Sea Res.* **13**, 707–730.

MUNK, W. H. 1981 Internal waves and small scale processes. In *Evolution of Physical Oceanography* (ed. B. A. Warren & C. Wunch), 264–291. MIT.

NASMYTH, P. W. 1970 Oceanic turbulence. Ph.D. dissertation, University of British Columbia.

OAKEY, N. S. & ELLIOTT, J. A. 1980 The variability of temperature gradient microstructure observed in the Denmark Strait. *J. Geophys. Res.* **85**, C4, 1933–1944.

SCHEDVIN, J. C. 1979 Microscale measurements of temperature in the upper ocean from a towed body. Ph.D. dissertation, University of California at San Diego.

STILLINGER, D. C. 1981 An experimental study of the transition of grid turbulence to internal waves in a salt-stratified water channel. Ph.D. dissertation, University of California at San Diego.

STILLINGER, D. C., HELLAND, K. N. & VAN ATTA, C. W. 1983 Experiments on the transition of homogeneous turbulence to internal waves in a stratified fluid. *J. Fluid Mech.* **131**, 91–122.

TURNER, J. S. 1973 *Buoyancy Effects in Fluids*. Cambridge University Press.

WASHBURN, L. & GIBSON, C. H. 1984 Horizontal variability of temperature microstructure in the seasonal thermocline during MILE. *J. Geophys. Res.* **89**, 3507–3522.

WILLIAMS, R. B. 1974 Direct measurements of turbulence in the Pacific Equatorial Undercurrent. Ph.D. dissertation, University of California at San Diego.

WOODS, J. D. (ed.), HOGSTROM, V., MISME, P., OTTERSTEN, H. & PHILLIPS, O. M. Report of working group: fossil turbulence. *Radio Sci.* **4**, 1365–1367.